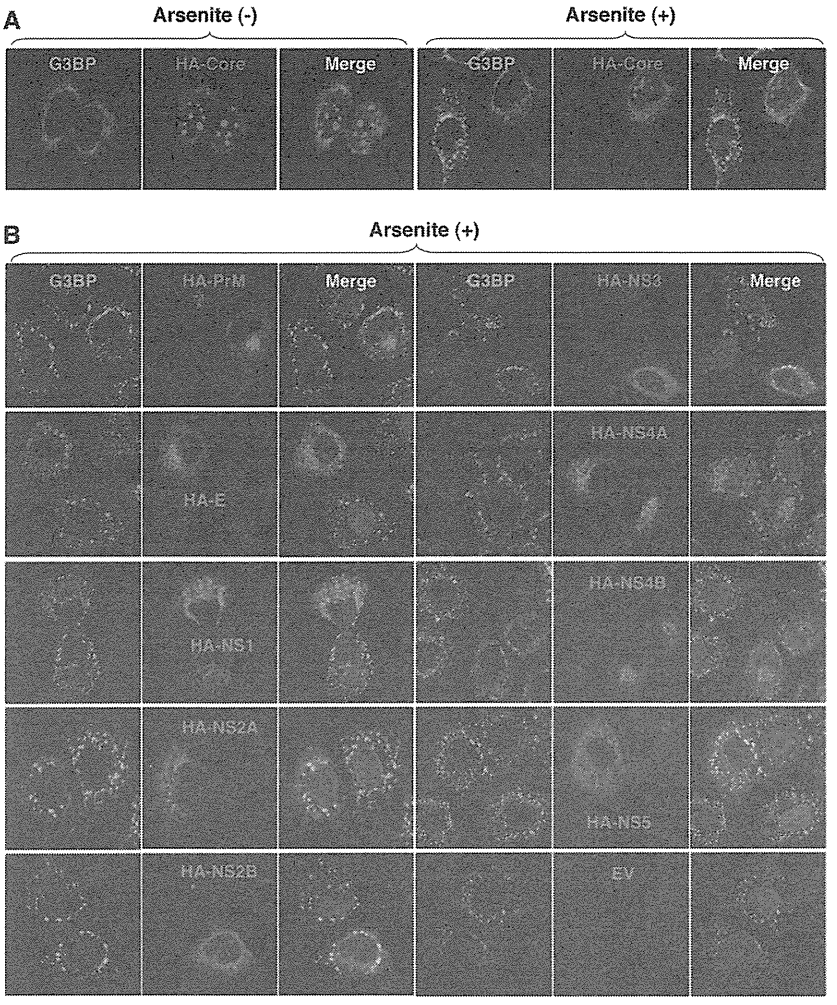

FIG 4 Inhibition of the arsenite-induced SG formation by the expression of JEV proteins. (A) Huh7 cells transfected with a plasmid, pCAGPM-HA-Core, were treated with or without 1.0 mM sodium arsenite for 30 min at 37°C, and the cellular localizations of G3BP and HA-Core were determined at 24 h posttransfection by immunofluorescence analysis with mouse anti-G3BP MAb and rat anti-HA MAb, followed by AF488-conjugated anti-mouse IgG and AF594-conjugated anti-rat IgG, respectively. Cell nuclei were stained with DAPI (blue). (B) Huh7 cells, which were separately transfected with a plasmid expressing an individual viral protein (pCAGPM-HA-JEV protein) as indicated in the figure, were treated with 1.0 mM sodium arsenite for 30 min at 37°C and subjected to an immunofluorescence assay using mouse anti-G3BP MAb and rat anti-HA MAb, followed by AF488-conjugated anti-mouse IgG and AF594-conjugated anti-rat IgG, respectively. Cell nuclei were stained with DAPI (blue).

formation induced by sodium arsenite, JEV-infected cells were treated with 0.5 mM sodium arsenite for 30 min at 24 h postinfection. Although many G3BP-positive foci were observed in mock-infected cells by the treatment with sodium arsenite, accumulation of G3BP in the perinuclear region was observed in the JEV-infected cells (Fig. 1A, right), and the numbers of G3BP-positive foci in the JEV-infected cells were less than those in the mock-infected cells (Fig. 1G). Although it has been reported that a significant reduction of the phosphorylation at Ser^{51} of eIF2α in cells treated with arsenite was induced by infection with WNV (15), the phosphorylation of eIF2α was slightly suppressed in the JEV-infected cells (Fig. 1C). Furthermore, while previous studies reported that Caprin-1 and TIA-1 were colocalized with dsRNA in cells infected with DENV (15, 26), no colocalization of G3BP or TIA-1 with the DENV core protein was observed in the present study (Fig. 3), suggesting that the mechanisms of the viral circumvention of SG formation in cells infected with JEV are different from those in cells infected with WNV and DENV.

JEV core protein suppresses SG formation induced by sodium arsenite. To elucidate the molecular mechanisms of suppression of SG formation induced by sodium arsenite during JEV infection, we tried to identify which viral protein(s) is responsible for the SG inhibition. Since G3BP was colocalized with JEV core protein, we first examined the involvement of the core protein in the perinuclear accumulation of G3BP and in the suppression of SG formation. The expression of JEV core protein alone induced the accumulation of G3BP in the perinuclear region (Fig. 4A, left panel) and suppressed sodium arsenite-induced SG formation (Fig. 4A, upper right cell in the right panel), similarly to JEV infection. In contrast, inhibition of SG formation induced by sodium arsenite was not observed in cells expressing other JEV proteins (Fig. 4B). These results suggest that JEV core protein is responsible for the circumvention of the SG formation observed in cells infected with JEV.

JEV core protein directly interacts with Caprin-1, an SG-associated cellular factor. Since JEV core protein was suggested to

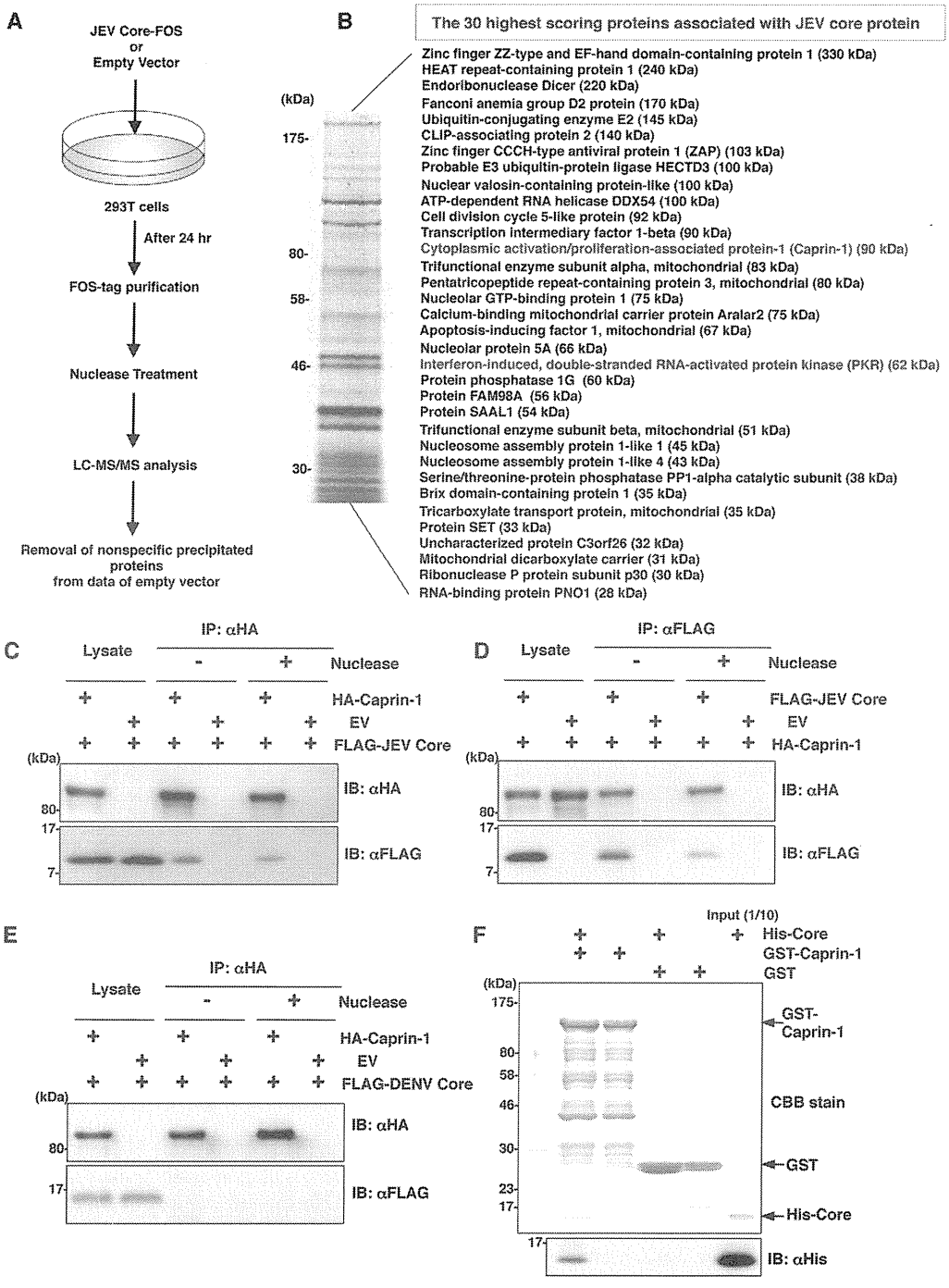

FIG 5 JEV core protein directly interacts with Caprin-1, an SG-associated cellular factor. (A) Identification of host cellular proteins associated with JEV core protein by FOS-tagged purification and LC-MS/MS analysis. Overview of the FOS-tagged purification of cellular proteins associated with JEV core protein. (B) The 30 candidate proteins as binding partners of JEV core protein exhibiting high scores are listed. PKR and Caprin-1 are indicated in red. (C and D) FLAG-JEV core protein and HA-Caprin-1 were coexpressed in 293T cells, and the cell lysates harvested at 24 h posttransfection were treated with or without micrococcal nuclease for 30 min at 37°C and immunoprecipitated (IP) with anti-HA (αHA) or anti-FLAG (αFLAG) antibody, as indicated. The precipitates were subjected to immunoblotting (IB) to detect coprecipitated counterparts. (E) FLAG-DENV core protein was coexpressed with HA-Caprin-1 in 293T cells, immunoprecipitated with anti-HA antibody, and immunoblotted with anti-HA or anti-FLAG antibody. (F) His-tagged JEV core protein was incubated with either GST-fused Caprin-1 or GST for 2 h at 4°C, and the precipitates obtained by GST pulldown assay were subjected to CBB staining and immunoblotting with anti-His antibody.

participate in the inhibition of SG formation, we tried to identify cellular factors associated with the core protein by LC-MS/MS analysis, as shown in Fig. 5A. Among the 30 factors with the best scores, two SG-associated proteins, PKR (Mascot search score, 206) and Caprin-1 (Mascot search score, 153), were identified as binding partners of JEV core protein (Fig. 5B). Although PABP1, hnRNP Q, Staufen, G3BP, and eIF4G were also identified, their scores were lower than those of PKR and Caprin-1. Because the

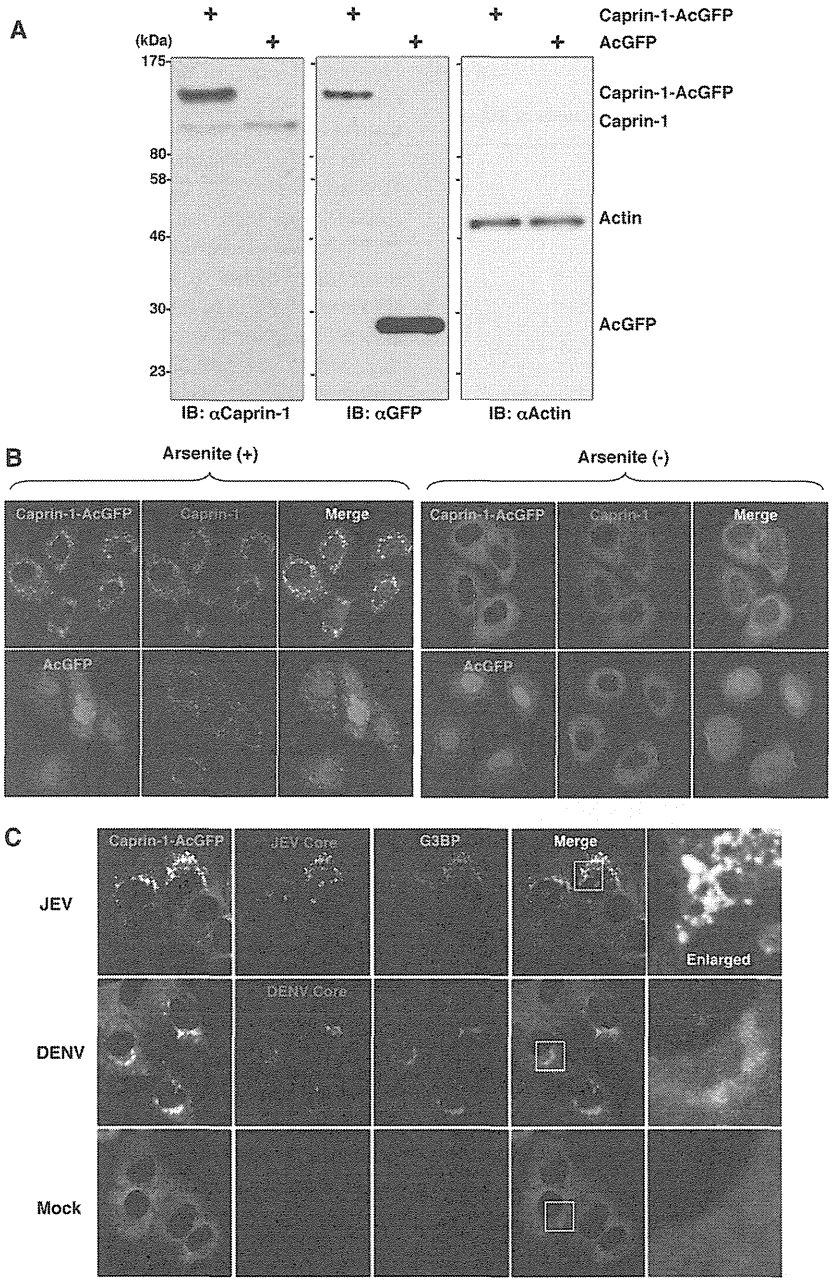

FIG 6 Caprin-1 is colocalized with the JEV core protein in the perinuclear region. (A) Expression of Caprin-1 fused with AcGFP (Caprin-1-AcGFP), Caprin-1, actin, or AcGFP in lentivirally transduced Huh7 cells was determined by immunoblotting using the appropriate antibodies. (B) Subcellular localization of Caprin-1-AcGFP or AcGFP (green) and endogenous Caprin-1 (red) in cells treated with/without 1.0 mM sodium arsenite for 30 min at 37°C was determined by immunofluorescence assay with rabbit anti-Caprin-1 PAb and AF594-conjugated anti-rabbit IgG. Cell nuclei were stained with DAPI (blue). (C) Huh7/Caprin-1-AcGFP cells were infected with either JEV or DENV at an MOI of 0.5, and the cellular localizations of JEV and DENV core (red) with Caprin-1-AcGFP and G3BP (blue) were determined at 24 h and 48 h postinfection, respectively. Cells were stained with mouse anti-G3BP MAb and rabbit anti-JEV or DENV core protein PAb, followed by AF633-conjugated anti-mouse IgG and AF594-conjugated anti-rabbit IgG, respectively, and examined by immunofluorescence analysis.

results shown in Fig. 1B suggest that the inhibition of SG formation takes place downstream of eIF2α phosphorylation, we focused on Caprin-1 as a key factor involved in the inhibition of SG formation in cells infected with JEV. To confirm the specific interaction of JEV core protein with Caprin-1, FLAG-JEV core protein and HA-Caprin-1 were coexpressed and immunoprecipitated with anti-HA or anti-FLAG antibody in the presence or absence of nuclease. FLAG-JEV core protein was coprecipitated with HA-Caprin-1 irrespective of nuclease treatment (Fig. 5C and D), suggesting that the interaction between JEV core protein and Caprin-1 is a protein-protein interaction. On the other hand, FLAG-DENV core protein was not coprecipitated with HA-Caprin-1 (Fig. 5E), indicating that the interaction with Caprin-1 was specific for JEV core protein. Next, the direct interaction be-

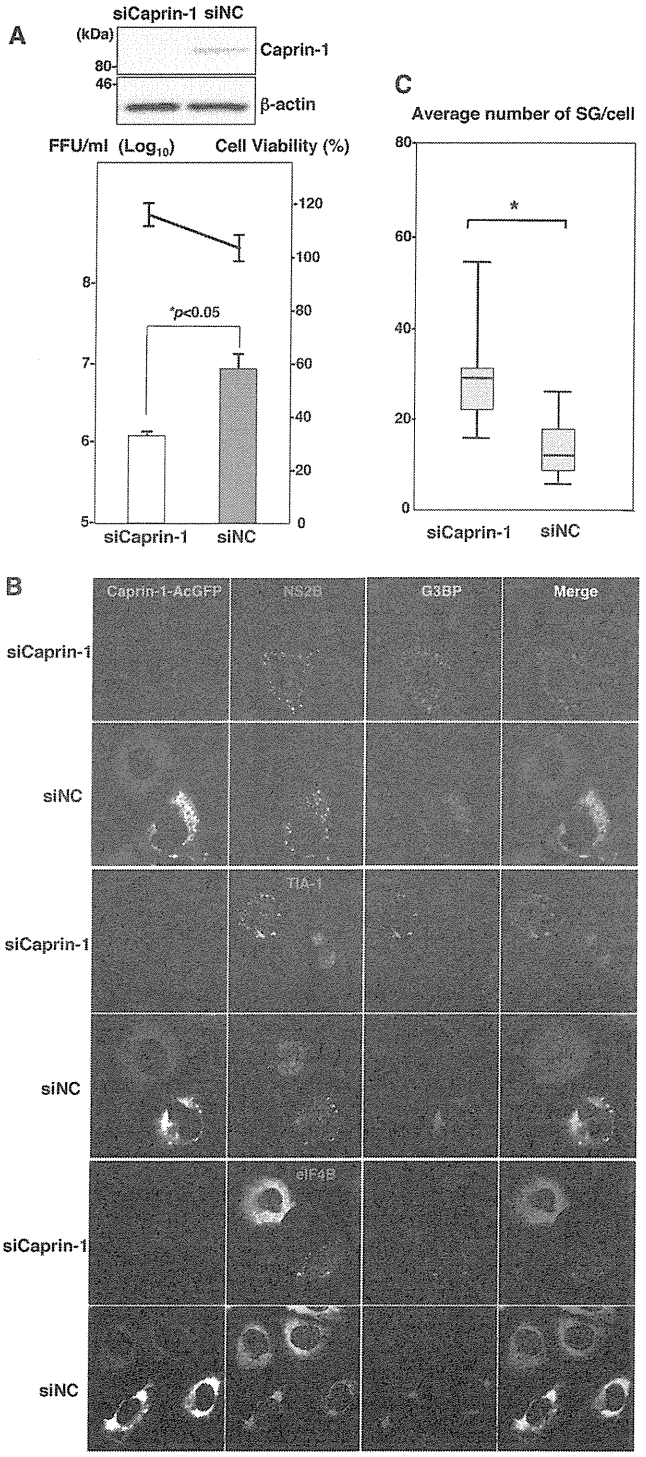

FIG 7 Knockdown of Caprin-1 cancels SG inhibition during JEV infection and suppresses viral propagation. (A) (Upper) The levels of expression of Caprin-1 in cells transfected with either siCaprin-1 or siNC was determined by immunoblotting using anti-Caprin-1 and anti-β-actin antibodies at 72 h posttransfection (top panel). At 48 h posttransfection with either siCaprin-1 or siNC, Huh7/Caprin-1-AcGFP cells were inoculated with JEV at an MOI of 0.5. At 24 h postinfection (72 h posttransfection), the infectious titers in the supernatants were determined by focus-forming assay in Vero cells (bottom panel, bar graph). Cell viability was determined at 72 h posttransfection and calculated as a percentage of the viability of cells treated with siNC (bottom panel, line graph). The results shown are from three independent assays, with the error bars representing the standard deviations. (B) At 48 h posttransfection with either siCaprin-1 or siNC, Huh7/Caprin-1-AcGFP cells were inoculated with JEV at an MOI of 0.5. The cellular localizations of SG-associated factors and JEV NS2B were determined at 24 h postinfection (72 h posttransfection) by immunofluorescence analysis with mouse anti-G3BP MAb and rabbit anti-NS2B PAb, rabbit anti-eIF4B PAb, or goat anti-TIA-1 PAb, followed by AF633-conjugated anti-mouse IgG and AF594-conjugated anti-rabbit IgG or AF594-conjugated anti-goat IgG, respectively. (C) Numbers of G3BP-positive foci in 30 cells prepared as described in panel B were counted. Lines, boxes, and error bars indicate the means, 25th to 75th percentiles, and 95th percentiles, respectively. The significance of differences between the means was determined by a Student's *t* test. *, $P < 0.01$.

tween JEV core protein and Caprin-1 was examined by a GST-pulldown assay using purified proteins expressed in bacteria. The His-tagged core protein was coprecipitated with GST-tagged Caprin-1, suggesting that JEV core protein directly interacts with Caprin-1 (Fig. 5F).

To further determine the cellular localization of Caprin-1 in JEV-infected cells, Caprin-1 fused with AcGFP (Caprin-1-AcGFP) was lentivirally expressed in Huh7 cells. The levels of expression and recruitment of Caprin-1-AcGFP into SGs were determined by immunoblotting and immunofluorescence analysis, respectively (Fig. 6A and B). In cells infected with JEV, Caprin-1-AcGFP was concentrated in the perinuclear region and colocalized with core protein and G3BP, while no colocalization of the proteins was observed in cells infected with DENV (Fig. 6C), suggesting that Caprin-1 directly interacts with JEV core protein in the perinuclear region of the infected cells.

Knockdown of Caprin-1 cancels SG inhibition during JEV infection and suppresses viral propagation. To assess the biological significance of the interaction of JEV core protein with Caprin-1 in JEV propagation, the expression of Caprin-1 was suppressed by using Caprin-1-specific siRNAs (siCaprin-1). Transfection of siCaprin-1 efficiently and specifically knocked down the expression of Caprin-1 with a slight increase of cell viability and decreased the production of infectious particles in the culture supernatants of cells infected with JEV, in comparison with those treated with a control siRNA (siNC) (Fig. 7A). Furthermore, immunofluorescence analyses revealed that knockdown of Caprin-1 increased the number of G3BP-positive granules colocalized with SG-associated factors, including TIA-1 and eIF4B, and inhibited the G3BP concentration in the perinuclear region (Fig. 7B and C). These results suggest that knockdown of Caprin-1 suppresses JEV propagation through the induction of SG formation.

Lys^{97} and Arg^{98} in the JEV core protein are crucial residues for the interaction with Caprin-1. To determine amino acid residues of the core protein that are required for the interaction with Caprin-1, we constructed a putative model based on the structural information of the DENV core protein previously resolved by nuclear magnetic resonance (NMR) (27), as shown in Fig. 8A. Based on this model, we selected hydrophobic amino acids, which were located on the solvent-exposed side in the α1 and α4 helices, as amino acid residues responsible for the binding to host proteins. Amino acid substitutions in each of the α-helices shown in Fig. 8B were designed in the context of FLAG-Core (Mα1 and Mα4), and the interaction of FLAG-Core mutants with Caprin-1 was examined by immunoprecipitation analysis. WT and Mα1, but not Mα4, core proteins were immunoprecipitated with Caprin-1 (Fig. 8B). To determine the amino acids responsible for interaction with Caprin-1, further alanine substitutions were introduced in the α4 helix, and the interaction was examined by immunopre-

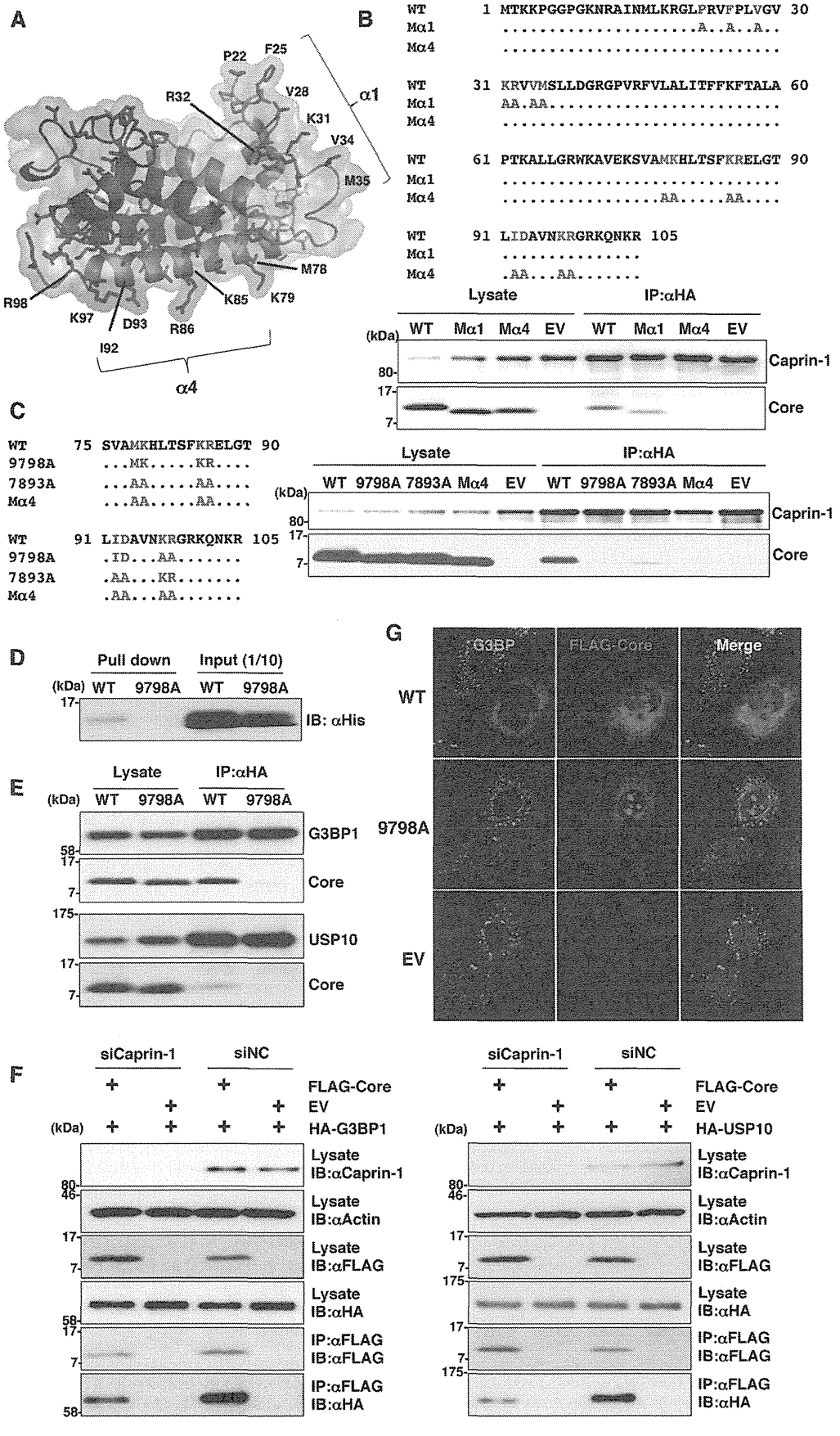

cipitation assay. As shown in Fig. 8C, double replacing both Lys^{97} and Arg^{98} with Ala (9798A) completely abrogated the interaction with Caprin-1. The importance of these two amino acids in the interaction with Caprin-1 was also confirmed by GST pulldown assay (Fig. 8D). These results indicate that Lys^{97} and Arg^{98} in the JEV core protein are crucial for the interaction with Caprin-1. Since G3BP has been reported to be one of the key molecules for SG formation and interacts with several SG component molecules including Caprin-1 and USP10 (28, 29), interactions of the core protein with SG components were examined by immunoprecipitation assay. The wild-type but not mutant 9798A core protein was associated with G3BP1 and USP10 (Fig. 8E). In addition, the knockdown of Caprin-1 weakened the interactions of core protein with G3BP1 or USP10 (Fig. 8F). These findings indicate that JEV core protein associates with several SG component molecules, such as G3BP1 and USP10, through the interaction with Caprin-1. Next, the role of the interaction between JEV core protein and Caprin-1 in the suppression of SG formation was examined by immunofluorescence analysis. Although the expression of the wild-type JEV core protein suppressed the SG formation induced by sodium arsenite treatment, as shown above, expression of the 9798A mutant did not (Fig. 8G), suggesting that the interaction of JEV core protein with Caprin-1 through Lys^{97} and Arg^{98} plays a crucial role in the inhibition of SG formation.

Interaction of the JEV core protein with Caprin-1 plays crucial roles not only in viral propagation *in vitro* but also in the pathogenesis in mice through the suppression of SG formation. To further examine the biological significance of the interaction between the JEV core protein and Caprin-1 in viral replication, we generated a mutant infectious cDNA clone (pMWJEAT/9798AA) of JEV encoding a mutant core protein deficient in the binding to Caprin-1 based on pMWJEAT. First, the cellular localization of the core protein in the 9798A mutant JEV-infected cells was examined by immunofluorescence analysis. The 9798A mutant core protein, as well as the wild-type core protein, was localized in the nucleus and the perinuclear region (Fig. 9A). However, the 9798A mutant core protein was not colocalized with Caprin-1, in contrast to the wild-type core protein. The sizes of infectious foci in Vero cells infected with the 9798A mutant were significantly smaller than those infected with the wild-type JEV (Fig. 9B). Furthermore, the infectious titers in C6/36 and Vero cells infected with the 9798A mutant were 6.1- and 12.6-fold lower than those infected with wild-type JEV at 48 h postinfection, respectively (Fig. 9C), suggesting that interaction of the JEV core protein with Caprin-1 plays crucial roles in the propagation of JEV in both insect and mammalian cells. Cells infected with the 9798A mutant induced SGs containing both G3BP and Caprin-1, in contrast to the accumulation of G3BP in the perinuclear region observed in those infected with the wild-type JEV (Fig. 9D). The numbers of foci in cells infected with the 9798A mutant were higher than those in cells infected with the wild-type JEV (Fig. 9E), indicating that the interaction of the JEV core protein with Caprin-1 is crucial for the suppression of SG formation. Finally, we examined the biological relevance of the interaction of JEV core protein with Caprin-1 in viral replication *in vivo*. Infectious particles were recovered from the cerebrums of ICR mice inoculated with wild-type JEV but not from those inoculated with the 9798A mutant (Fig. 9F). In addition, all 10 mice had died by 12 days postinoculation with the wild-type JEV, while only 1 mouse had died at day 10 postinoculation with the 9798A mutant (Fig. 9G). Collectively, these results suggest that the interaction of JEV core protein with Caprin-1 plays crucial roles not only in viral replication *in vitro* but also in pathogenesis in mice through the suppression of SG formation.

DISCUSSION

Viruses are obligatory intracellular parasites, and their life cycles rely on host cellular functions. Many viruses have evolved to inhibit SG formation and thereby evade the host translation shutoff mechanism and facilitate viral replication (6, 30), while some viruses co-opt molecules regulating SG formation for viral replication (11, 31). The vaccinia virus subverts SG components to generate aggregates containing G3BP, Caprin-1, eIF4G, eIF4E, and mRNA of the virus, but not of the host, in order to stimulate viral translation (11). Replication, translation, and assembly of transmissible gastroenteritis coronavirus, a member of the *Coronaviridae* family, are regulated by the interaction of polypyrimidine tract-binding protein and TIA-1 with viral RNA (31). HIV-1 utilizes Staufen1, which is a principal component of SG, in the viral RNA selection to form ribonucleoproteins (RNPs) through interaction with Gag protein, instead of SG translation silencing (8). In the case of flaviviruses, TIA-1 and TIAR bind to the 3′ untranslated region (UTR) of the negative-stranded RNA of WNV to facilitate viral replication (16), and G3BP1, Caprin-1, and USP10 interact with DENV RNA, although the biological significance of these interactions remains unknown (26). In this study, we have shown that JEV infection suppresses SG formation by the recruitment of several effector molecules promoting SG assembly, including G3BP and USP10, to the perinuclear region through the interaction of JEV core protein with Caprin-1. Furthermore, a mutant JEV carrying a core protein incapable of binding to

FIG 8 Lys^{97} and Arg^{98} in the JEV core protein are crucial residues for the interaction with Caprin-1. (A) Putative structural model of the core protein homodimer of JEV deduced from that of DENV obtained from the Protein Data Bank (accession number 1R6R) by using PyMOL software. The two α helices (α1 and α4) are indicated. (B) FLAG-Core mutants in which the hydrophobic amino acid residues in the α1 helix (Mα1) or α4 helix (Mα4) were replaced with alanine were coexpressed with HA-Caprin-1 in 293T cells, immunoprecipitated (IP) with anti-HA antibody, and examined by immunoblotting (IB) with anti-HA or anti-FLAG antibody. (C) FLAG-Core mutants in which the Met^{78}, Lys^{79}, Lys^{85}, Arg^{86}, Ile^{92}, and Asp^{93} (7893A) or Lys^{97} and Arg^{98} (9798A) in the α4 helix domain were replaced with alanine were coexpressed with HA-Caprin-1 in 293T cells and examined as described in panel B. (D) The His-tagged JEV core protein (WT or 9798A) was incubated with GST-fused Caprin-1 for 2 h at 4°C, and the precipitates obtained by GST pulldown assay were subjected to immunoblotting with anti-His antibody. (E) FLAG-Core (WT or 9798A) was coexpressed with HA-G3BP1 or HA-USP10 in 293T cells, immunoprecipitated with anti-HA antibody, and immunoblotted with anti-HA and anti-FLAG antibodies. (F) FLAG-JEV Core was coexpressed with HA-G3BP1 or HA-USP10 in 293T cells transfected with either siCaprin-1 or siNC at 72 h posttransfection, immunoprecipitated with anti-FLAG antibody, and immunoblotted with anti-HA and anti-FLAG antibodies. The cell lysates were also subjected to immunoblotting with anti-Caprin-1 and anti-β-actin antibodies to evaluate the knockdown efficiency of Caprin-1. (G) The cellular localizations of G3BP and FLAG-Core (WT or 9798A) were determined at 24 h posttransfection after treatment with 1.0 mM sodium arsenite for 30 min at 37°C by immunofluorescence analysis with mouse anti-G3BP MAb and rabbit anti-FLAG PAb, followed by AF488-conjugated anti-mouse IgG and AF594-conjugated anti-rabbit IgG, respectively. Cell nuclei were stained with DAPI (blue).

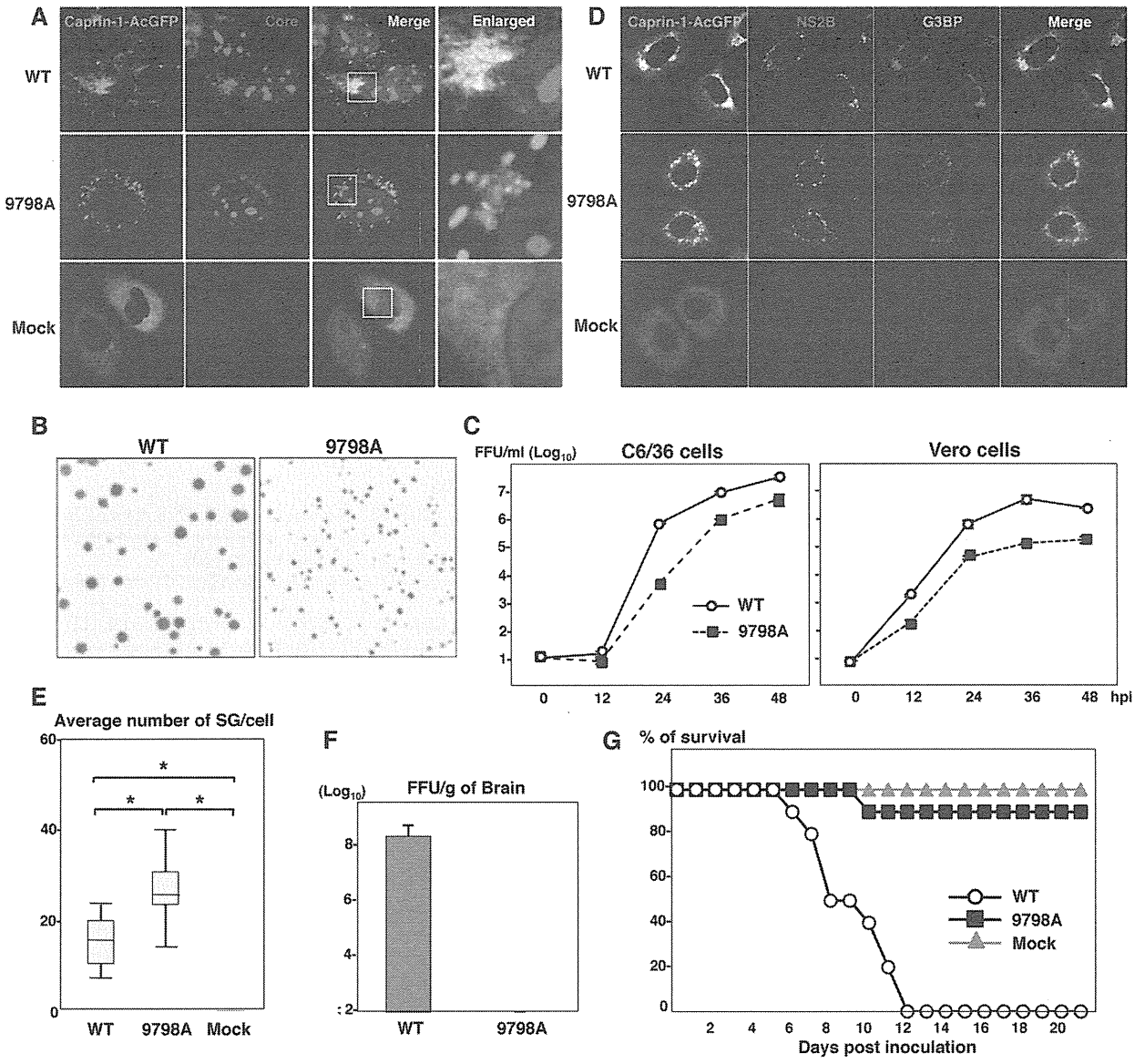

FIG 9 Interaction of JEV core protein with Caprin-1 plays crucial roles not only in viral replication *in vitro* but also in pathogenesis in mice through the suppression of SG formation. (A) Huh7/Caprin-1-AcGFP cells were infected with JEV (WT or 9798A mutant) at an MOI of 1.0, and the cellular localizations of Caprin-1-AcGFP and JEV core protein were determined at 24 h postinfection by immunofluorescence analysis with rabbit anti-core PAb and AF594-conjugated anti-rabbit IgG. Cell nuclei were stained with DAPI (blue). (B) Focus formation of JEV (WT or 9798A mutant) in Vero cells incubated in methylcellulose overlay medium at 48 h postinfection. The infectious foci were immunostained as described previously (20). (C) Growth kinetics of JEV (WT or 9798A mutant) in C6/36 and Vero cells infected at an MOI of 0.1. Infectious titers in the culture supernatants harvested at the indicated times were determined by focus-forming assays in Vero cells. Means of three experiments are indicated. (D) Huh7/Caprin-1-AcGFP cells were infected with either WT or 9798A at an MOI of 0.5, and cellular localizations of Caprin-1-AcGFP, G3BP (blue), and JEV NS2B (red) were determined at 24 h postinfection by immunofluorescence analysis with mouse anti-G3BP MAb and rabbit anti-NS2B PAb, followed by AF633-conjugated anti-mouse IgG and AF594-conjugated anti-rabbit IgG, respectively. (E) Numbers >of G3BP-positive foci in 30 cells prepared as described in panel D were counted. Lines, boxes, and error bars indicate the means, 25th to 75th percentiles, and 95th percentiles, respectively. The significance of differences between the means was determined by Student's *t* test. *, $P < 0.01$. (F) Infectious titers in the cerebrums of mice at 7 days postintraperitoneal inoculation with 5×10^4 FFU/100 μl of either WT or 9798A virus were determined in Vero cells. The means of titers in the homogenates of the cerebrums from three mice are indicated. The detection limit is 10^2 FFU/g of cerebrum. (G) Percentages of surviving mice ($n = 10$) after intraperitoneal inoculation with 5×10^4 FFU of either WT or 9798A virus. Mock, inoculation with DMEM.

Caprin-1 exhibited reduced replication *in vitro* and attenuated pathogenicity in mice.

G3BP is one of the key molecules involved in the SG aggregation process and self-oligomerizes in a phosphorylation-dependent manner to sequester mRNA in SGs (4). Therefore, G3BP knocked down cells (6) and G3BP knockout mouse embryonic fibroblast cells are deficient in the SG formation. In addition, G3BP sequestration inhibits SG formation in response to arsenite treatment (32). Caprin-1, known as RNA granule protein 105 or p137 (33), also participates in SG formation through phosphorylation of eIF2α (28) and is ubiquitously expressed in the cytoplasm. Caprin-1 regulates the transport and translation of mRNAs

of proteins involved in the synaptic plasticity in neurons (34) and cellular proliferation and migration in multiple cell types (28) through an interaction with G3BP. USP10, another SG-associated molecule, also interacts with G3BP and forms the G3BP/USP10 complex (29), suggesting that several SG-associated RBPs participate in the formation of a protein-protein network. In this study, the JEV core protein was shown to directly interact with Caprin-1, to sequester several key molecule complexes involved in SG formation to the perinuclear region in cells infected with JEV, and to facilitate viral propagation through the suppression of SG formation.

Flaviviruses replicate at a relatively low rate in comparison with most of the other positive-stranded RNA viruses, and thus rapid shutdown of host cellular protein synthesis would be deleterious for the viral life cycle. In cells infected with JEV, several SG components were colocalized with the core protein in the perinuclear region, while in those infected with WNV or DENV, SG components were accumulated in a replication complex composed of viral RNA and nonstructural proteins. In addition, the phosphorylation of eIF2α induced by arsenite was completely canceled by the infection with WNV or DENV, whereas the suppression of the phosphorylation was limited in JEV infection (15). Incorporation of the nascent viral RNA into the membranous structure induced by viral nonstructural proteins prevents PKR activation and inhibits SG formation in cells infected with WNV (17). In cells infected with hepatitis C virus (HCV), which belongs to the genus *Hepacivirus* in the family *Flaviviridae*, induction of SG formation was observed in the early stage of infection, in contrast to the inhibition of the arsenite-induced SG formation in the late stage (35). Several SG components, such as G3BP1, PABP1, and ataxin-2, were colocalized with HCV core protein around lipid droplets (35), and G3BP1 was also associated with the NS5B protein and the 5′ terminus of the minus-strand viral RNA (36) to mediate efficient viral replication. Collectively, these data suggest that flaviviruses have evolved to regulate cellular processes involved in SG formation through various strategies.

PKR is one of the interferon-stimulated genes and plays a crucial role in antiviral defense through phosphorylation of eIF2α, which leads to host translational shutoff (37, 38). In the early stage of flavivirus infection, both positive- and negative-stranded RNAs transcribe at low levels, while genomic RNA predominantly synthesizes in the late stage of infection (39). It was shown that activation of PKR was suppressed (40) or only induced in the late stage of WNV infection (41) and impaired by the expression of HCV NS5A (42–44). Very recently, JEV NS2A was shown to suppress PKR activation through inhibition of dimerization of PKR in the early stage but not in the late stage of infection (45). In this study, we have shown that JEV core protein interacts with Caprin-1 and inhibits SG formation downstream of the phosphorylation of eIF2α in the late stage of infection, suggesting that JEV has evolved to escape from host antiviral responses in the multiple stages of viral replication by using structural and nonstructural proteins.

The flavivirus core protein is a multifunctional protein involved in many aspects of the viral life cycle. In addition to the formation of viral nucleocapsid through the interaction with viral RNA (as a structural protein) (46), flavivirus core proteins interact with various host factors, such as B23 (47), Jab1 (48), hnRNP K (49), and hnRNP A2 (23), and regulate viral replication and/or modify the host cell environment (as a nonstructural protein). Although further investigations are needed to clarify the precise mechanisms underlying the circumvention of SG formation through the interaction of JEV core protein with Caprin-1, leading to efficient propagation *in vitro* and pathogenicity in mice, these findings could help not only to provide new insight into strategies by which viruses escape host stress responses but also to develop novel antiviral agents for flavivirus infection.

ACKNOWLEDGMENTS

We thank M. Tomiyama for secretarial assistance. We also thank K. Saito and T. Wakita for technical advice and the infectious clone of JEV, respectively.

This work was supported in part by grants-in-aid from the Ministry of Health, Labor, and Welfare, the Ministry of Education, Culture, Sports, Science, and Technology, and the Osaka University Global Center of Excellence Program. H. Katoh is a research fellow of the Japanese Society for the Promotion of Science.

REFERENCES

1. **Nover L, Scharf KD, Neumann D.** 1989. Cytoplasmic heat shock granules are formed from precursor particles and are associated with a specific set of mRNAs. Mol. Cell. Biol. **9**:1298–1308.
2. **Anderson P, Kedersha N.** 2002. Stressful initiations. J. Cell Sci. **115**:3227–3234.
3. **Gilks N, Kedersha N, Ayodele M, Shen L, Stoecklin G, Dember LM, Anderson P.** 2004. Stress granule assembly is mediated by prion-like aggregation of TIA-1. Mol. Biol. Cell **15**:5383–5398.
4. **Tourriere H, Chebli K, Zekri L, Courselaud B, Blanchard JM, Bertrand E, Tazi J.** 2003. The RasGAP-associated endoribonuclease G3BP assembles stress granules. J. Cell Biol. **160**:823–831.
5. **Kedersha N, Cho MR, Li W, Yacono PW, Chen S, Gilks N, Golan DE, Anderson P.** 2000. Dynamic shuttling of TIA-1 accompanies the recruitment of mRNA to mammalian stress granules. J. Cell Biol. **151**:1257–1268.
6. **White JP, Cardenas AM, Marissen WE, Lloyd RE.** 2007. Inhibition of cytoplasmic mRNA stress granule formation by a viral proteinase. Cell Host Microbe **2**:295–305.
7. **Khaperskyy DA, Hatchette TF, McCormick C.** 2012. Influenza A virus inhibits cytoplasmic stress granule formation. FASEB J. **26**:1629–1639.
8. **Abrahamyan LG, Chatel-Chaix L, Ajamian L, Milev MP, Monette A, Clement JF, Song R, Lehmann M, DesGroseillers L, Laughrea M, Boccaccio G, Mouland AJ.** 2010. Novel Staufen1 ribonucleoproteins prevent formation of stress granules but favour encapsidation of HIV-1 genomic RNA. J. Cell Sci. **123**:369–383.
9. **McInerney GM, Kedersha NL, Kaufman RJ, Anderson P, Liljestrom P.** 2005. Importance of eIF2α phosphorylation and stress granule assembly in alphavirus translation regulation. Mol. Biol. Cell **16**:3753–3763.
10. **Smith JA, Schmechel SC, Raghavan A, Abelson M, Reilly C, Katze MG, Kaufman RJ, Bohjanen PR, Schiff LA.** 2006. Reovirus induces and benefits from an integrated cellular stress response. J. Virol. **80**:2019–2033.
11. **Katsafanas GC, Moss B.** 2007. Colocalization of transcription and translation within cytoplasmic poxvirus factories coordinates viral expression and subjugates host functions. Cell Host Microbe **2**:221–228.
12. **Misra UK, Kalita J.** 2010. Overview: Japanese encephalitis. Prog. Neurobiol. **91**:108–120.
13. **Sumiyoshi H, Mori C, Fuke I, Morita K, Kuhara S, Kondou J, Kikuchi Y, Nagamatu H, Igarashi A.** 1987. Complete nucleotide sequence of the Japanese encephalitis virus genome RNA. Virology **161**:497–510.
14. **Murray CL, Jones CT, Rice CM.** 2008. Architects of assembly: roles of *Flaviviridae* non-structural proteins in virion morphogenesis. Nat. Rev. Microbiol. **6**:699–708.
15. **Emara MM, Brinton MA.** 2007. Interaction of TIA-1/TIAR with West Nile and dengue virus products in infected cells interferes with stress granule formation and processing body assembly. Proc. Natl. Acad. Sci. U. S. A. **104**:9041–9046.
16. **Li W, Li Y, Kedersha N, Anderson P, Emara M, Swiderek KM, Moreno GT, Brinton MA.** 2002. Cell proteins TIA-1 and TIAR interact with the 3′ stem-loop of the West Nile virus complementary minus-strand RNA and facilitate virus replication. J. Virol. **76**:11989–12000.
17. **Courtney SC, Scherbik SV, Stockman BM, Brinton MA.** 2012. West Nile

virus infections suppress early viral RNA synthesis and avoid inducing the cell stress granule response. J. Virol. 86:3647–3657.
18. Kambara H, Tani H, Mori Y, Abe T, Katoh H, Fukuhara T, Taguwa S, Moriishi K, Matsuura Y. 2011. Involvement of cyclophilin B in the replication of Japanese encephalitis virus. Virology 412:211–219.
19. Mori Y, Yamashita T, Tanaka Y, Tsuda Y, Abe T, Moriishi K, Matsuura Y. 2007. Processing of capsid protein by cathepsin L plays a crucial role in replication of Japanese encephalitis virus in neural and macrophage cells. J. Virol. 81:8477–8487.
20. Mori Y, Okabayashi T, Yamashita T, Zhao Z, Wakita T, Yasui K, Hasebe F, Tadano M, Konishi E, Moriishi K, Matsuura Y. 2005. Nuclear localization of Japanese encephalitis virus core protein enhances viral replication. J. Virol. 79:3448–3458.
21. Kambara H, Fukuhara T, Shiokawa M, Ono C, Ohara Y, Kamitani W, Matsuura Y. 2012. Establishment of a novel permissive cell line for the propagation of hepatitis C virus by expression of microRNA miR122. J. Virol. 86:1382–1393.
22. Zhao Z, Date T, Li Y, Kato T, Miyamoto M, Yasui K, Wakita T. 2005. Characterization of the E-138 (Glu/Lys) mutation in Japanese encephalitis virus by using a stable, full-length, infectious cDNA clone. J. Gen. Virol. 86:2209–2220.
23. Katoh H, Mori Y, Kambara H, Abe T, Fukuhara T, Morita E, Moriishi K, Kamitani W, Matsuura Y. 2011. Heterogeneous nuclear ribonucleoprotein A2 participates in the replication of Japanese encephalitis virus through an interaction with viral proteins and RNA. J. Virol. 85:10976–10988.
24. Hamamoto I, Nishimura Y, Okamoto T, Aizaki H, Liu M, Mori Y, Abe T, Suzuki T, Lai MM, Miyamura T, Moriishi K, Matsuura Y. 2005. Human VAP-B is involved in hepatitis C virus replication through interaction with NS5A and NS5B. J. Virol. 79:13473–13482.
25. Jones CT, Ma L, Burgner JW, Groesch TD, Post CB, Kuhn RJ. 2003. Flavivirus capsid is a dimeric alpha-helical protein. J. Virol. 77:7143–7149.
26. Ward AM, Bidet K, Yinglin A, Ler SG, Hogue K, Blackstock W, Gunaratne J, Garcia-Blanco MA. 2011. Quantitative mass spectrometry of DENV-2 RNA-interacting proteins reveals that the DEAD-box RNA helicase DDX6 binds the DB1 and DB2 3′ UTR structures. RNA Biol. 8:1173–1186.
27. Ma L, Jones CT, Groesch TD, Kuhn RJ, Post CB. 2004. Solution structure of dengue virus capsid protein reveals another fold. Proc. Natl. Acad. Sci. U. S. A. 101:3414–3419.
28. Solomon S, Xu Y, Wang B, David MD, Schubert P, Kennedy D, Schrader JW. 2007. Distinct structural features of Caprin-1 mediate its interaction with G3BP-1 and its induction of phosphorylation of eukaryotic translation initiation factor 2α, entry to cytoplasmic stress granules, and selective interaction with a subset of mRNAs. Mol. Cell. Biol. 27:2324–2342.
29. Soncini C, Berdo I, Draetta G. 2001. Ras-GAP SH3 domain binding protein (G3BP) is a modulator of USP10, a novel human ubiquitin specific protease. Oncogene 20:3869–3879.
30. Montero H, Rojas M, Arias CF, Lopez S. 2008. Rotavirus infection induces the phosphorylation of eIF2α but prevents the formation of stress granules. J. Virol. 82:1496–1504.
31. Sola I, Galan C, Mateos-Gomez PA, Palacio L, Zuniga S, Cruz JL, Almazan F, Enjuanes L. 2011. The polypyrimidine tract-binding protein affects coronavirus RNA accumulation levels and relocalizes viral RNAs to novel cytoplasmic domains different from replication-transcription sites. J. Virol. 85:5136–5149.
32. Hinton SD, Myers MP, Roggero VR, Allison LA, Tonks NK. 2010. The pseudophosphatase MK-STYX interacts with G3BP and decreases stress granule formation. Biochem. J. 427:349–357.
33. Grill B, Wilson GM, Zhang KX, Wang B, Doyonnas R, Quadroni M, Schrader JW. 2004. Activation/division of lymphocytes results in increased levels of cytoplasmic activation/proliferation-associated protein-1: prototype of a new family of proteins. J. Immunol. 172:2389–2400.
34. Shiina N, Shinkura K, Tokunaga M. 2005. A novel RNA-binding protein in neuronal RNA granules: regulatory machinery for local translation. J. Neurosci. 25:4420–4434.
35. Ariumi Y, Kuroki M, Kushima Y, Osugi K, Hijikata M, Maki M, Ikeda M, Kato N. 2011. Hepatitis C virus hijacks P-body and stress granule components around lipid droplets. J. Virol. 85:6882–6892.
36. Yi Z, Pan T, Wu X, Song W, Wang S, Xu Y, Rice CM, Macdonald MR, Yuan Z. 2011. Hepatitis C virus co-opts Ras-GTPase-activating protein-binding protein 1 for its genome replication. J. Virol. 85:6996–7004.
37. Gale M, Jr, Katze MG. 1998. Molecular mechanisms of interferon resistance mediated by viral-directed inhibition of PKR, the interferon-induced protein kinase. Pharmacol. Ther. 78:29–46.
38. Pindel A, Sadler A. 2011. The role of protein kinase R in the interferon response. J. Interferon Cytokine Res. 31:59–70.
39. Chu PW, Westaway EG. 1985. Replication strategy of Kunjin virus: evidence for recycling role of replicative form RNA as template in semiconservative and asymmetric replication. Virology 140:68–79.
40. Elbahesh H, Scherbik SV, Brinton MA. 2011. West Nile virus infection does not induce PKR activation in rodent cells. Virology 421:51–60.
41. Samuel MA, Whitby K, Keller BC, Marri A, Barchet W, Williams BR, Silverman RH, Gale M, Jr, Diamond MS. 2006. PKR and RNase L contribute to protection against lethal West Nile Virus infection by controlling early viral spread in the periphery and replication in neurons. J. Virol. 80:7009–7019.
42. Gale M, Jr, Blakely CM, Kwieciszewski B, Tan SL, Dossett M, Tang NM, Korth MJ, Polyak SJ, Gretch DR, Katze MG. 1998. Control of PKR protein kinase by hepatitis C virus nonstructural 5A protein: molecular mechanisms of kinase regulation. Mol. Cell. Biol. 18:5208–5218.
43. Gale MJ, Jr, Korth MJ, Tang NM, Tan SL, Hopkins DA, Dever TE, Polyak SJ, Gretch DR, Katze MG. 1997. Evidence that hepatitis C virus resistance to interferon is mediated through repression of the PKR protein kinase by the nonstructural 5A protein. Virology 230:217–227.
44. He Y, Tan SL, Tareen SU, Vijaysri S, Langland JO, Jacobs BL, Katze MG. 2001. Regulation of mRNA translation and cellular signaling by hepatitis C virus nonstructural protein NS5A. J. Virol. 75:5090–5098.
45. Tu YC, Yu CY, Liang JJ, Lin E, Liao CL, Lin YL. 2012. Blocking dsRNA-activated protein kinase PKR by Japanese encephalitis virus nonstructural protein 2A. J. Virol. 86:10347–10358.
46. Khromykh AA, Westaway EG. 1996. RNA binding properties of core protein of the flavivirus Kunjin. Arch. Virol. 141:685–699.
47. Tsuda Y, Mori Y, Abe T, Yamashita T, Okamoto T, Ichimura T, Moriishi K, Matsuura Y. 2006. Nucleolar protein B23 interacts with Japanese encephalitis virus core protein and participates in viral replication. Microbiol. Immunol. 50:225–234.
48. Oh W, Yang MR, Lee EW, Park KM, Pyo S, Yang JS, Lee HW, Song J. 2006. Jab1 mediates cytoplasmic localization and degradation of West Nile virus capsid protein. J. Biol. Chem. 281:30166–30174.
49. Chang CJ, Luh HW, Wang SH, Lin HJ, Lee SC, Hu ST. 2001. The heterogeneous nuclear ribonucleoprotein K (hnRNP K) interacts with dengue virus core protein. DNA Cell Biol. 20:569–577.

J Gastroenterol (2013) 48:169–176
DOI 10.1007/s00535-012-0661-5

REVIEW

Role of miR-122 and lipid metabolism in HCV infection

Takasuke Fukuhara · Yoshiharu Matsuura

Received: 6 August 2012 / Accepted: 7 August 2012 / Published online: 11 September 2012

Abstract Hepatitis C virus (HCV) exhibits a narrow host range and a specific tissue tropism. Mice expressing major entry receptors for HCV permit viral entry, and therefore the species tropism of HCV infection is considered to be reliant on the expression of the entry receptors. However, HCV receptor candidates are expressed and replication of HCV-RNA can be detected in several nonhepatic cell lines, suggesting that nonhepatic cells are also susceptible to HCV infection. Recently it was shown that the exogenous expression of a liver-specific microRNA, miR-122, facilitated the efficient replication of HCV not only in hepatic cell lines, including Hep3B and HepG2 cells, but also in nonhepatic cell lines, including Hec1B and HEK-293T cells, suggesting that miR-122 is required for the efficient replication of HCV in cultured cells. However, no infectious particle was detected in the nonhepatic cell lines, in spite of the efficient replication of HCV-RNA. In the nonhepatic cells, only small numbers of lipid droplets and low levels of very-low-density lipoprotein-associated proteins were observed compared with findings in the hepatic cell lines, suggesting that functional lipid metabolism participates in the assembly of HCV. Taken together, these findings indicate that miR-122 and functional lipid metabolism are involved in the tissue tropism of HCV infection. In this review, we would like to focus on the role of miR-122 and lipid metabolism in the cell tropism of HCV.

T. Fukuhara · Y. Matsuura (✉)
Department of Molecular Virology,
Research Institute for Microbial Diseases, Osaka University,
3-1 Yamada-oka, Suita, Osaka 565-0871, Japan
e-mail: matsuura@biken.osaka-u.ac.jp

Keywords HCV · miR-122 · Lipid metabolism

Introduction

More than 170 million individuals worldwide are chronically infected with hepatitis C virus (HCV), and the cirrhosis and hepatocellular carcinoma (HCC) induced by HCV infection are life-threatening diseases [1]. On the other hand, HCV infection sometimes induces extra-hepatic manifestations (EHM), including mixed cryoglobulinemia and non-Hodgkin lymphoma [2–5]. The mechanisms of the pathogenesis and cell tropism of HCV have not been fully elucidated yet owing to the lack of an appropriate infection model. Although chimpanzees are susceptible to HCV infection, the use of these animals to study experimental infection is ethically problematic, and no other animal model with susceptibility to HCV infection has been established [6]. Furthermore, robust in vitro HCV propagation has been limited to the combination of cell-culture-adapted clones based on the genotype 2a JFH1 strain (HCVcc) and human liver cancer-derived Huh7 cells [7, 8]. The expression of a liver-specific microRNA, miR-122, has been shown to dramatically enhance the translation and replication of HCV-RNA [9]. Recently, several reports have shown that the exogenous expression of miR-122 facilitates the efficient replication of viral RNA in several hepatic and nonhepatic cell lines [10–13]. Of note, the clinical application of a specific inhibitor of miR-122 to chronic hepatitis C patients is now in progress [14]. In addition, it has been shown that liver-specific expression of very-low-density lipoprotein (VLDL)-associated proteins is involved in the assembly of infectious HCV particles [15, 16]. This review will focus on the role of miR-122 expression and lipid metabolism in HCV infection.

microRNA and virus infection

miRNAs were first identified by Lee et al. [17] and since that time a great number of miRNAs have been registered in the miRNA database. miRNA incorporated into RNA-induced silencing complex (RISC) interacts with a target mRNA via a specific recognition element. RISC contains argonaute 2 (Ago2), Dicer, and TAR RNA binding protein (TRBP) [18, 19]. In humans, Ago2 plays a pivotal role in the repression of translation of target genes [20]. It is now commonly believed that miRNAs play important roles in cell homeostasis, and that abnormality of miRNA expression participates in the development of several diseases, including viral infections [18, 19]. miRNAs encoded by Epstein–Barr virus (EBV) were identified in 2004 [4, 21], and over 200 viral miRNAs have been reported in several DNA viruses, especially in herpesviruses [22, 23]. Previous reports have shown that viral miRNAs participate in viral propagation by regulating the host gene expression [22, 23]. Many viral miRNAs suppress the host gene expression involved in innate and acquired immunities and enhance viral propagation [22, 24, 25]. Most RNA viruses replicate in the cytoplasm, and thus it had been believed that RNA viruses do not encode viral miRNAs. Rouha et al. [26] showed that an RNA virus, the tick-borne encephalitis virus, is capable of producing functional miRNA by the insertion of an miRNA element into viral RNA. Actually, it has been shown that virus-derived small RNAs emerge by infection with RNA viruses, including influenza virus and West Nile virus [27, 28]. These data suggest that both viral-encoded and host gene-derived miRNAs are involved in the regulation of viral propagation.

Liver-specific microRNA, miR-122

miR-122 is a liver-specific microRNA and is the microRNA most abundantly expressed in the liver [29–31]. Although Li et al. [32] have suggested that hepatocyte nuclear factor 4 alpha (HNF4A) positively regulates the expression of miR-122, the details on the tissue specificity of miR-122 expression have not been fully elucidated yet. miR-122 targets the 3′untranslated region (3′UTR) of the mRNAs of cytoplasmic polyadenylation element binding protein (CPEB), hemochromatosis (Hfe), hemojuverin (Hjv), disintegrin, and metalloprotease family 10 (ADAM10) and represses their translation [33–35]. miR-122 activates the translation of p53 mRNA through the suppression of CPEB and participates in cellular senescence [33]. Through the inhibition of Hfe and Hjv, miR-122 participates in iron metabolism [34]. Esau et al. [36] showed that miR-122 positively regulated lipid metabolism through the reduction of the mRNAs of lipid-associated proteins, and that inhibition of miR-122 expression attenuated liver steatosis in high-fat-fed mice, suggesting that miR-122 may be an attractive therapeutic target for metabolic diseases. miR-122 has also been shown to be involved in the propagation of hepatitis viruses, including hepatitis B virus (HBV) and HCV [9, 37, 38]. Wang et al. [38] have revealed that miR-122 suppresses cyclin G1, and this factor is known to enhance the replication of HBV by inhibiting the binding of p53 to HBV enhancer elements. In other reports, a low level of miR-122 expression in plasma was significantly associated with the incidence of HBV-related HCC [39]. These results suggest that miR-122 expression inhibits the propagation and pathogenesis of HBV. On the other hand, miR-122 expression enhances the propagation of HCV through genetic interaction with the 5′UTR of the HCV genome [9]. It is interesting to note that the effects of miR-122 expression on viral propagation are different between HBV and HCV.

miR-122 expression and HCV infection (Fig. 1)

Jopling et al. [9] reported for the first time that the inhibition of miR-122 dramatically decreased RNA replication in HCV replicon cells harboring subgenomic (SGR) or fullgenomic (FGR) viral RNA. They identified the 21 nucleotide (nt) of the miR-122 binding site in the 5′ end of the 5′UTR of HCV RNA. In addition, lack of enhancement of HCV replication by the expression of a mutant miR-122 incapable of binding to the 5′UTR was canceled by the introduction of a complementary mutation in the 5′UTR, suggesting that direct interaction of miR-122 with the 5′UTR is crucial for the enhancement of HCV replication. In subsequent reports, they identified a second adjacent miR-122 binding site in the 5′UTR [40]. Furthermore, ectopic expression of the mutant miR-122 rescued the replication of an HCV RNA possessing mutations in both miR-122 binding sites, suggesting that the interaction of miR-122 with both sites in the 5′UTR is required to augment viral replication. In addition, Machlin et al. [41] have revealed that not only the seed sequence but also nucleotides located at the positions of 15 and 16 in miR-122 are required for the enhancement of HCV replication. Interestingly, nucleotides 15 and 16 are not required for the conventional microRNA function of miR-122, suggesting that the conventional machinery of miR-122 is not involved in the miR-122-dependent enhancement of HCV replication. A recent study showed that the interaction of miR-122 with the 5′UTR of HCV was also required for the efficient production of infectious particles in cell culture [42].

Although the precise mechanisms of the miR-122-mediated enhancement of HCV replication have not been

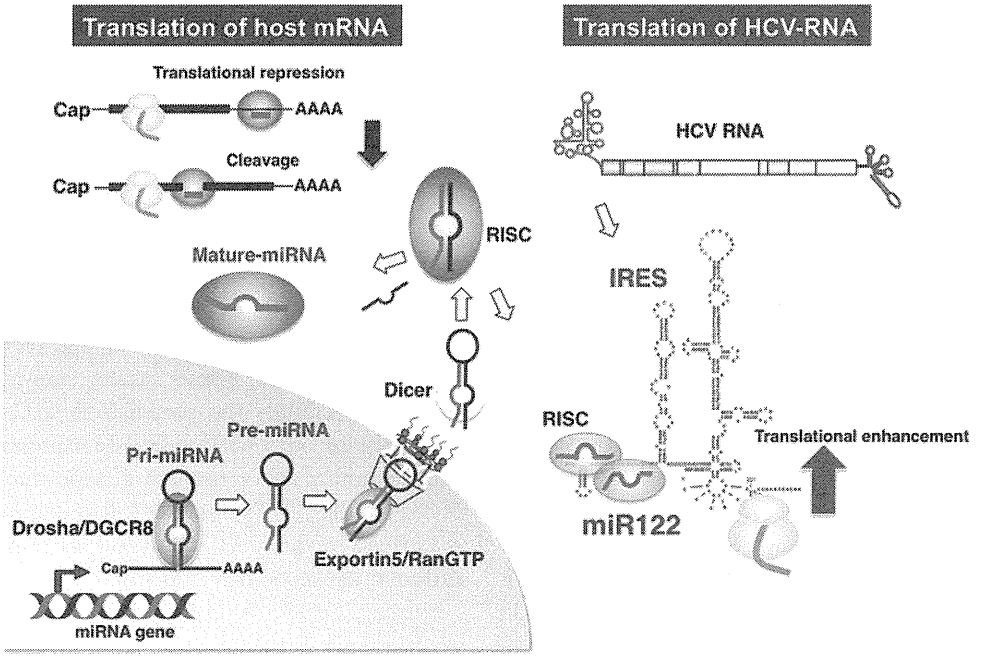

Fig. 1 miR-122 enhances the translation of hepatitis C virus (*HCV*) RNA. Primary miRNA (*pri-miRNA*) transcribed by RNA polymerase II in the nucleus is processed into precursor miRNA (*pre-miRNA*) by Drosha and DiGeorge syndrome critical region protein 8 (*DGCR8*). Pre-miRNA is exported into the cytoplasm by nucleocytoplasmic shuttle protein exportin 5, processed to 22nt by dicer, and then incorporated into argonaute proteins to form the RNA-induced silencing complex (*RISC*). The passenger strand of miRNA (*blue*) is degraded and the guide strand (*red*) is matured in the RISC. Generally, miRNA represses the translation of host mRNA by binding to its 3'untranslated region (3′UTR). In contrast, liver-specific miR-122 binds to two sites in the 5′UTR of the HCV genome and enhances its translation and replication. *GTP* Guanosine-5-triphosphate, *IRES* internal ribosomal entry site

fully elucidated yet, Henke et al. [43], by using polymerase defective viral RNA, showed that miR-122 stimulated the translation of HCV RNA by enhancing the association of ribosomes at an early initiation stage. They concluded that miR-122 might contribute to HCV liver tropism at the level of translation. Wilson et al. [44] showed that knockdown of Ago2 in SGR cells and HCVcc-infected cells attenuated HCV replication, and that knockdown of Ago2 also reduced the translation of the polymerase defective HCV RNA. Shimakami et al. [45] showed that miR-122 stabilized viral RNA and reduced its decay in concert with Ago2, and that miR-122-dependent stabilization of HCV RNA was not observed in Ago2-knockout murine embryonic fibroblasts. These results suggest that Ago2 is required for the efficient enhancement of both the translation and replication of HCV. On the other hand, Machlin et al. [41] have suggested that the 3′ overhang binding of miR-122 to the 5′ end of the HCV genome participates in circumvention from the recognition by the cytoplasmic RNA sensor, RIG-I. It is feasible to speculate that miR-122 has other functions in the HCV life cycle, in addition to the stabilization of viral RNA and evasion from the host's innate immune response.

Establishment of new permissive cell lines for HCV propagation by the expression of miR-122

The lack of immunocompetent small animal models and cell culture systems to support the propagation of HCV in patient sera has hampered both the understanding of the HCV life cycle and the development of antiviral drugs [46]. HCV replicon cells in which the HCV genome autonomously replicates, and pseudotype viruses bearing HCV E1 and E2 glycoproteins were established to assess viral replication and entry, respectively [47, 48]. Afterwards, an infectious HCV derived from the JFH1 strain of genotype 2a (HCVcc) was developed [7, 8]. On the basis of the data obtained from these in vitro systems, the HCV life cycle has been clarified, and host factors involved in HCV propagation have been identified as therapeutic targets for chronic hepatitis C [46]. However, the robust propagation of HCVcc in well-characterized human liver cell lines other than Huh7 had not been successful until recently. Chang et al. [49] showed that the exogenous expression of miR-122 facilitated the replication of HCV RNA in kidney-derived HEK-293 cells. In addition, Lin et al. have demonstrated that the expression of miR-122 and depletion of interferon regulatory factor 3 (IRF-3) permit replication

of the HCV genome in mouse fibroblasts [50]. These results suggest that the expression of miR-122 might facilitate the efficient replication of HCVcc not only in hepatic cells but also in nonhepatic cells. In fact, the expression level of miR-122 in Huh7 cells has been shown to be higher than that in other hepatic cell lines, including Huh6, HepG2, and Hep3B cells [10]. Recently, two groups reported that miR-122 expression facilitated the efficient propagation of HCVcc in human hepatic cell lines [10, 11]. Narbus et al. [11] showed that HepG2 cells stably expressing CD81 and miR-122 supported efficient replication and the production of infectious particles. Interestingly, internal ribosomal entry site (IRES)-dependent translation of HCV exhibited a slight (1.4–2.1-fold) increase by the expression of miR-122 in HepG2 cells compared with that in parental cells, suggesting that miR-122 is required for efficient RNA replication but not in translation in HepG2 cells upon infection with HCVcc. Kambara et al. [10] established a novel permissive cell line for the propagation of HCVcc by the expression of miR-122 in Hep3B cells. miR-122 expression facilitated the efficient propagation of HCVcc and the establishment of HCV replicon cells in Hep3B cells. In addition, "cured" Hep3B cells established by the elimination of HCV RNA from the Hep3B replicon cells facilitated the efficient propagation of HCVcc compared to parental cells. Interestingly, the expression of miR-122 in the "cured" Hep3B cells was significantly higher than that in the parental cells. In addition, Ehrhadt et al. [51] have shown that the expression levels of miR-122 in Huh7-derived cured cells, including Huh7.5 and Huh-Lunet cells, are significantly higher than those in parental Huh7 cells. Collectively, these results suggest that miR-122 is a key determinant of the efficient replication of HCVcc in hepatic cell lines.

Expression of miR-122 facilitates the efficient replication of HCV in nonhepatic cells

In clinical studies, negative strands of HCV genome have been detected in nonhepatic tissues of chronic hepatitis C patients, suggesting the possibility of extrahepatic propagation of HCV [52–56]. In addition, HCV replication was detected in peripheral blood mononuclear cells (PBMCs) of patients with occult HCV infection [57]. Roque-Afonso et al. [52] showed that highly divergent variants of HCV were detectable in PBMCs, but not in plasma or in liver, suggesting the possibility of the extrahepatic propagation of HCV. Furthermore, previous reports have suggested that recurrences of HCV infection after antiviral treatment or liver transplantation were attributable to chronic infection of HCV in extrahepatic tissues [58]. Collectively, these results might suggest a correlation between extrahepatic HCV replication and the development of EHM, including mixed cryoglobulinemia and non-Hodgkin lymphoma, which are frequently observed in chronic hepatitis C patients. However, details of the extrahepatic propagation of HCV have not been studied owing to the lack of an appropriate experimental model [59, 60].

HCV replicon cells have been established in several nonhepatic cell lines. Kato et al. [61] established JFH1-based SGR cells by using HeLa and HEK293 cells, suggesting that the HCV genome can replicate in nonhepatic cells. In addition, Fletcher et al. [62] showed that brain endothelial cells supported HCV entry and replication, suggesting that HCV infection in the central nervous system participates in HCV-associated neuropathologies. Given the marked effects of miR-122 expression on the propagation of HCVcc in hepatic cell lines, we hypothesized that the expression of miR-122 in nonhepatic cell lines would facilitate the establishment of novel permissive cell lines for HCV. Recently, we have shown that Hec1B cells derived from the human uterus exhibited a low level of viral replication and the exogenous expression of miR-122 significantly enhanced replication upon infection with HCVcc [63]. In addition, an miR-122-specific inhibitor for miR-122 called locked nucleic acid (LNA-miR-122) inhibited the enhancement of HCVcc replication in Hec1B cells expressing miR-122, while the basal replication of HCVcc in parental Hec1B cells was resistant to the treatment. These results suggest that Hec1B cells permit HCV replication in an miR-122-independent manner and the exogenous expression of miR-122 enhances viral replication. In this report, cured Hec1B cells established by the elimination of HCV RNA from Hec1B replicon cells exhibited more potent replication of HCVcc than the parental cells. As seen in the cured Hep3B cells, the expression levels of miR-122 in the Hec1B cured cells were significantly higher than those in the parental cells [63]. Taken together, these results show that the expression of miR-122 facilitates the replication of HCVcc in nonhepatic cells.

Viral assembly in nonhepatic cells

Previous reports have shown that the production of VLDL is involved in the formation of infectious HCV particles [15, 16]. Apolipoprotein B (ApoB), apolipoprotein E (ApoE), and microsomal triglyceride transfer protein (MTTP) have major roles in the secretion of VLDL. Gastaminza et al. [15] have demonstrated that ApoB and MTTP are cellular factors essential for the efficient assembly of infectious HCV particles. They concluded that HCV acquired hepatocyte tropism through utilization of the VLDL secretory pathway. On the other hand, studies by

other groups have demonstrated that infectious HCV particles are highly enriched in ApoE, which is a major determinant of HCV infectivity and production [64]. In their reports, small interfering RNA (siRNA)-mediated knockdown of ApoB and treatment with MTTP inhibitors exhibited no significant effect on the infectivity and production of HCV, suggesting that ApoE but not ApoB is required for viral assembly. In addition, Mancone et al. [65] have shown that apolipoprotein A-I (ApoA-I) is required for the replication of HCV and the production of infectious particles. Collectively, these results suggest that several VLDL-associated proteins are involved in HCV assembly.

In our recent report, the viral assembly process was shown to be impaired in nonhepatic cells exogenously expressing miR-122, in spite of the efficient replication of the HCV genome [63]. Interestingly, low but substantial infectious titers were detected in hepatic Hep3B cells upon infection with HCVcc, even though the RNA replication was lower than that in nonhepatic Hec1B cells expressing miR-122. The expression levels of VLDL-associated proteins, including ApoE, ApoB, and MTTP, in nonhepatic cell lines were significantly lower than those in hepatic cell lines, suggesting that lack of expression of VLDL-associated proteins is one of the reasons for the inability of nonhepatic cells to produce infectious particles. Miyanari et al. [66] showed that lipid droplets (LDs) were required for the formation of infectious particles via interaction between the core protein and viral RNA. Interestingly, only a small amount of LDs was detected in nonhepatic cells, including Hec1B and HEK293T cells, compared with the amount in hepatic cell lines, suggesting that a low level of LD formation is also involved in the impairment of infectious particle formation in nonhepatic cells [63]. Taken together, these findings suggest the possibility that the reconstitution of functional lipid metabolism in nonhepatic cells facilitates the production of infectious particles.

Tropism of HCV infection

In many cases, the cell tropism of viral infection is defined by the expression of virus-specific receptors. The expression of CD4 and chemokine receptors has an important role in the determination of the lymphotropism of human immunodeficiency virus infection [67]. In measles virus infection, the signaling lymphocyte activation molecule is a determinant of lymphotropism [68, 69]. Previous reports have shown that human CD81, scavenger receptor class B1 (SR-B1), Claudin1 (CLDN1), and Occludin (OCLN) are crucial for HCV entry [70–73]. Although murine cells cannot permit HCV entry, the exogenous expression of human-derived receptor candidates in murine cells has been shown to facilitate HCV entry, suggesting that HCV-specific receptors participate in the determination of the cell tropism of HCV [74, 75]. However, previous reports have also revealed that HCV receptor candidates were highly expressed in many nonhepatic tissues [62, 76], and our recent report has demonstrated that many nonhepatic cells permit the entry of HCV pseudotypes [63]. In addition, many reports have suggested the possibility of HCV replication in extrahepatic sites such as PBMCs and neuronal cells [55, 62], suggesting that host factors other than receptors could be involved in the tissue tropism of HCV.

Although previous reports have shown that host factors such as VAMP-associated protein (VAP)-A, VAP-B, cyclophilin A, FK506 binding protein 8, and heat shock protein 90 participate in HCV replication, these molecules are unlikely to participate in the determination of the liver tropism of HCV, owing to their ubiquitous expression [46, 77–79]. As described above, miR-122 is abundantly expressed specifically in hepatocytes and is essential for the efficient replication of HCV. In addition, a recent report showed that hepatocyte-like cells derived from induced pluripotent stem cells (iPSCs) expressed high levels of miR-122 and supported the entire life cycle of HCVcc, suggesting that miR-122 might be one of the most critical determinants of the liver tropism of HCV infection [80, 81]. On the other hand, VLDL-associated proteins,

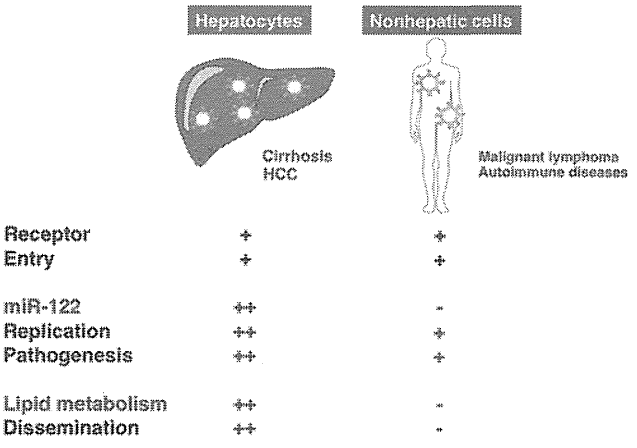

Fig. 2 HCV replication in hepatocytes and nonhepatic cells. Chronic HCV infection induces liver cirrhosis and hepatocellular carcinoma (*HCC*), and is also often associated with the development of extrahepatic manifestations (EHM) such as malignant lymphoma and autoimmune diseases. Not only hepatocytes but also nonhepatic cells express major HCV receptors, including CD81, SR-BI, CLDN1, and OCLN. In hepatocytes, functional expression of miR-122 and lipid metabolism facilitate the efficient propagation of HCV. In contrast, the lack of expression of miR-122 and very-low-density lipoprotein (VLDL)-associated proteins might be associated with the incomplete propagation of HCV in nonhepatic cells. Low levels of HCV replication in nonhepatic cells may participate in the development of EHM

including ApoB, ApoE, and MTTP, are specifically expressed in hepatic cells, and no infectious particles are produced in nonhepatic cells such as Hec1B and 293T-CLDN cells [63]. Collectively, these data suggest that the VLDL-producing system is involved in the liver tropism of HCV.

Although HCV can internalize not only into hepatocytes but also into nonhepatic cells through receptor-mediated endocytosis, miR-122 expression and functional lipid metabolism in hepatocytes facilitate the efficient replication and assembly of HCV (Fig. 2). On the other hand, lack of expression of miR-122 and VLDL-associated proteins might be associated with the incomplete propagation of HCV in nonhepatic cells (Fig. 2).

Conclusion

Recent progress in HCV research has revealed that the tissue tropism of HCV is reliant on the expression of liver-specific miR-122 and a functional lipid metabolism rather than being reliant on the expression of entry receptors. However, the molecular mechanisms of the enhancement of viral replication induced by the interaction of miR-122 with the 5′UTR of HCV and the assembly of viral particles via VLDL-producing machinery remain unknown. In addition, the participation of nonhepatic cells in the development of EHM has been suggested, through an incomplete or low level of HCV replication. Elucidation of the liver tropism of HCV will provide a clue to the development of new antiviral drugs for the treatment of chronic hepatitis C and could lead to an understanding of the pathogenesis of EHM induced by HCV infection.

Conflict of interest The authors declare that they have no conflicts of interest.

References

1. Seeff LB. Natural history of chronic hepatitis C. Hepatology. 2002;36:S35–46.
2. Hartridge-Lambert SK, Stein EM, Markowitz AJ, Portlock CS. Hepatitis C and non-Hodgkin lymphoma: the clinical perspective. Hepatology. 2012;55:634–41.
3. Calleja JL, Albillos A, Moreno-Otero R, Rossi I, Cacho G, Domper F, et al. Sustained response to interferon-alpha or to interferon-alpha plus ribavirin in hepatitis C virus-associated symptomatic mixed cryoglobulinaemia. Aliment Pharmacol Ther. 1999;13:1179–86.
4. Gumber SC, Chopra S. Hepatitis C: a multifaceted disease. Review of extrahepatic manifestations. Ann Intern Med. 1995;123:615–20.
5. Galossi A, Guarisco R, Bellis L, Puoti C. Extrahepatic manifestations of chronic HCV infection. J Gastrointest Liver Dis. 2007;16:65–73.
6. Bukh J. A critical role for the chimpanzee model in the study of hepatitis C. Hepatology. 2004;39:1469–75.
7. Wakita T, Pietschmann T, Kato T, Date T, Miyamoto M, Zhao Z, et al. Production of infectious hepatitis C virus in tissue culture from a cloned viral genome. Nat Med. 2005;11:791–6.
8. Lindenbach BD, Evans MJ, Syder AJ, Wolk B, Tellinghuisen TL, Liu CC, et al. Complete replication of hepatitis C virus in cell culture. Science. 2005;309:623–6.
9. Jopling CL, Yi M, Lancaster AM, Lemon SM, Sarnow P. Modulation of hepatitis C virus RNA abundance by a liver-specific microRNA. Science. 2005;309:1577–81.
10. Kambara H, Fukuhara T, Shiokawa M, Ono C, Ohara Y, Kamitani W, et al. Establishment of a novel permissive cell line for the propagation of hepatitis C virus by expression of microRNA miR122. J Virol. 2012;86:1382–93.
11. Narbus CM, Israelow B, Sourisseau M, Michta ML, Hopcraft SE, Zeiner GM, et al. HepG2 cells expressing microRNA miR-122 support the entire hepatitis C virus life cycle. J Virol. 2011;85:12087–92.
12. Sainz B Jr, Barretto N, Yu X, Corcoran P, Uprichard SL. Permissiveness of human hepatoma cell lines for HCV infection. Virol J. 2012;9:30.
13. Fukuhara T, Tani H, Shiokawa M, Goto Y, Abe T, Taketomi A, et al. Intracellular delivery of serum-derived hepatitis C virus. Microbes Infect. 2011;13:405–12.
14. Lanford RE, Hildebrandt-Eriksen ES, Petri A, Persson R, Lindow M, Munk ME, et al. Therapeutic silencing of microRNA-122 in primates with chronic hepatitis C virus infection. Science. 2010;327:198–201.
15. Gastaminza P, Cheng G, Wieland S, Zhong J, Liao W, Chisari FV. Cellular determinants of hepatitis C virus assembly, maturation, degradation, and secretion. J Virol. 2008;82:2120–9.
16. Cun W, Jiang J, Luo G. The C-terminal alpha-helix domain of apolipoprotein E is required for interaction with nonstructural protein 5A and assembly of hepatitis C virus. J Virol. 2010;84:11532–41.
17. Lee RC, Feinbaum RL, Ambros V. The *C. elegans* heterochronic gene lin-4 encodes small RNAs with antisense complementarity to lin-14. Cell. 1993;75:843–54.
18. Bartel DP. MicroRNAs: target recognition and regulatory functions. Cell. 2009;136:215–33.
19. Huntzinger E, Izaurralde E. Gene silencing by microRNAs: contributions of translational repression and mRNA decay. Nat Rev Genet. 2011;12:99–110.
20. Hutvagner G, Simard MJ. Argonaute proteins: key players in RNA silencing. Nat Rev Mol Cell Biol. 2008;9:22–32.
21. Pfeffer S, Zavolan M, Grasser FA, Chien M, Russo JJ, Ju J, et al. Identification of virus-encoded microRNAs. Science. 2004;304:734–6.
22. Boss IW, Renne R. Viral miRNAs and immune evasion. Biochim Biophys Acta. 2011;1809:708–14.
23. Ziegelbauer JM. Functions of Kaposi's sarcoma-associated herpesvirus microRNAs. Biochim Biophys Acta. 2011;1809:623–30.
24. Umbach JL, Kramer MF, Jurak I, Karnowski HW, Coen DM, Cullen BR. MicroRNAs expressed by herpes simplex virus 1 during latent infection regulate viral mRNAs. Nature. 2008;454:780–3.
25. Nachmani D, Stern-Ginossar N, Sarid R, Mandelboim O. Diverse herpesvirus microRNAs target the stress-induced immune ligand MICB to escape recognition by natural killer cells. Cell Host Microbe. 2009;5:376–85.
26. Rouha H, Thurner C, Mandl CW. Functional microRNA generated from a cytoplasmic RNA virus. Nucl Acids Res. 2010;38:8328–37.
27. Perez JT, Varble A, Sachidanandam R, Zlatev I, Manoharan M, Garcia-Sastre A, et al. Influenza A virus-generated small RNAs regulate the switch from transcription to replication. Proc Natl Acad Sci USA. 2010;107:11525–30.

28. Hussain M, Torres S, Schnettler E, Funk A, Grundhoff A, Pijlman GP, et al. West Nile virus encodes a microRNA-like small RNA in the 3′ untranslated region which up-regulates GATA4 mRNA and facilitates virus replication in mosquito cells. Nucl Acids Res. 2012;40:2210–23.
29. Lagos-Quintana M, Rauhut R, Yalcin A, Meyer J, Lendeckel W, Tuschl T. Identification of tissue-specific microRNAs from mouse. Curr Biol. 2002;12:735–9.
30. Chang J, Provost P, Taylor JM. Resistance of human hepatitis delta virus RNAs to dicer activity. J Virol. 2003;77:11910–7.
31. Chang J, Nicolas E, Marks D, Sander C, Lerro A, Buendia MA, et al. miR-122, a mammalian liver-specific microRNA, is processed from hcr mRNA and may downregulate the high affinity cationic amino acid transporter CAT-1. RNA Biol. 2004; 1:106–13.
32. Li ZY, Xi Y, Zhu WN, Zeng C, Zhang ZQ, Guo ZC, et al. Positive regulation of hepatic miR-122 expression by HNF4alpha. J Hepatol. 2011;55:602–11.
33. Burns DM, D'Ambrogio A, Nottrott S, Richter JD. CPEB and two poly(A) polymerases control miR-122 stability and p53 mRNA translation. Nature. 2011;473:105–8.
34. Castoldi M, Vujic Spasic M, Altamura S, Elmen J, Lindow M, Kiss J, et al. The liver-specific microRNA miR-122 controls systemic iron homeostasis in mice. J Clin Invest. 2011; 121:1386–96.
35. Bai S, Nasser MW, Wang B, Hsu SH, Datta J, Kutay H, et al. MicroRNA-122 inhibits tumorigenic properties of hepatocellular carcinoma cells and sensitizes these cells to sorafenib. J Biol Chem. 2009;284:32015–27.
36. Esau C, Davis S, Murray SF, Yu XX, Pandey SK, Pear M, et al. miR-122 regulation of lipid metabolism revealed by in vivo antisense targeting. Cell Metab. 2006;3:87–98.
37. Qiu L, Fan H, Jin W, Zhao B, Wang Y, Ju Y, et al. miR-122-induced down-regulation of HO-1 negatively affects miR-122-mediated suppression of HBV. Biochem Biophys Res Commun. 2010;398:771–7.
38. Wang S, Qiu L, Yan X, Jin W, Wang Y, Chen L, et al. Loss of microRNA 122 expression in patients with hepatitis B enhances hepatitis B virus replication through cyclin G(1)-modulated P53 activity. Hepatology. 2012;55:730–41.
39. Zhou J, Yu L, Gao X, Hu J, Wang J, Dai Z, et al. Plasma microRNA panel to diagnose hepatitis B virus-related hepatocellular carcinoma. J Clin Oncol. 2011;29:4781–8.
40. Jopling CL, Schutz S, Sarnow P. Position-dependent function for a tandem microRNA miR-122-binding site located in the hepatitis C virus RNA genome. Cell Host Microbe. 2008;4:77–85.
41. Machlin ES, Sarnow P, Sagan SM. Masking the 5′ terminal nucleotides of the hepatitis C virus genome by an unconventional microRNA-target RNA complex. Proc Natl Acad Sci USA. 2011;108:3193–8.
42. Shimakami T, Yamane D, Welsch C, Hensley L, Jangra RK, Lemon SM. Base pairing between hepatitis C virus RNA and microRNA 122 3′ of its seed sequence is essential for genome stabilization and production of infectious virus. J Virol. 2012;86:7372–83.
43. Henke JI, Goergen D, Zheng J, Song Y, Schuttler CG, Fehr C, et al. MicroRNA-122 stimulates translation of hepatitis C virus RNA. EMBO J. 2008;27:3300–10.
44. Wilson JA, Zhang C, Huys A, Richardson CD. Human Ago2 is required for efficient microRNA 122 regulation of hepatitis C virus RNA accumulation and translation. J Virol. 2011;85:2342–50.
45. Shimakami T, Yamane D, Jangra RK, Kempf BJ, Spaniel C, Barton DJ, et al. Stabilization of hepatitis C virus RNA by an Ago2-miR-122 complex. Proc Natl Acad Sci USA. 2012; 109:941–6.
46. Moriishi K, Matsuura Y. Host factors involved in the replication of hepatitis C virus. Rev Med Virol. 2007;17:343–54.
47. Lohmann V, Korner F, Koch J, Herian U, Theilmann L, Bartenschlager R. Replication of subgenomic hepatitis C virus RNAs in a hepatoma cell line. Science. 1999;285:110–3.
48. Bartosch B, Dubuisson J, Cosset FL. Infectious hepatitis C virus pseudo-particles containing functional E1–E2 envelope protein complexes. J Exp Med. 2003;197:633–42.
49. Chang J, Guo JT, Jiang D, Guo H, Taylor JM, Block TM. Liver-specific microRNA miR-122 enhances the replication of hepatitis C virus in nonhepatic cells. J Virol. 2008;82:8215–23.
50. Lin LT, Noyce RS, Pham TN, Wilson JA, Sisson GR, Michalak TI, et al. Replication of subgenomic hepatitis C virus replicons in mouse fibroblasts is facilitated by deletion of interferon regulatory factor 3 and expression of liver-specific microRNA 122. J Virol. 2010;84:9170–80.
51. Ehrhardt M, Leidinger P, Keller A, Baumert T, Diez J, Meese E, et al. Profound differences of microRNA expression patterns in hepatocytes and hepatoma cell lines commonly used in hepatitis C virus studies. Hepatology. 2011;54:1112–3
52. Roque-Afonso AM, Ducoulombier D, Di Liberto G, Kara R, Gigou M, Dussaix E, et al. Compartmentalization of hepatitis C virus genotypes between plasma and peripheral blood mononuclear cells. J Virol. 2005;79:6349–57.
53. Zehender G, De Maddalena C, Bernini F, Ebranati E, Monti G, Pioltelli P, et al. Compartmentalization of hepatitis C virus quasispecies in blood mononuclear cells of patients with mixed cryoglobulinemic syndrome. J Virol. 2005;79:9145–56.
54. Blackard JT, Kemmer N, Sherman KE. Extrahepatic replication of HCV: insights into clinical manifestations and biological consequences. Hepatology. 2006;44:15–22.
55. Laskus T, Operskalski EA, Radkowski M, Wilkinson J, Mack WJ, deGiacomo M, et al. Negative-strand hepatitis C virus (HCV) RNA in peripheral blood mononuclear cells from anti-HCV-positive/HIV-infected women. J Infect Dis. 2007; 195:124–33.
56. Fletcher NF, Wilson GK, Murray J, Hu K, Lewis A, Reynolds GM, et al. Hepatitis C virus infects the endothelial cells of the blood-brain barrier. Gastroenterology. 2012;142:634–43 e6.
57. Castillo I, Rodriguez-Inigo E, Bartolome J, de Lucas S, Ortiz-Movilla N, Lopez-Alcorocho JM, et al. Hepatitis C virus replicates in peripheral blood mononuclear cells of patients with occult hepatitis C virus infection. Gut. 2005;54:682–5.
58. Laskus T, Radkowski M, Wilkinson J, Vargas H, Rakela J. The origin of hepatitis C virus reinfecting transplanted livers: serum-derived versus peripheral blood mononuclear cell-derived virus. J Infect Dis. 2002;185:417–21.
59. Ito M, Masumi A, Mochida K, Kukihara H, Moriishi K, Matsuura Y, et al. Peripheral B cells may serve as a reservoir for persistent hepatitis C virus infection. J Innate Immun. 2010;2:607–17.
60. Ramirez S, Perez-Del-Pulgar S, Carrion JA, Costa J, Gonzalez P, Massaguer A, et al. Hepatitis C virus compartmentalization and infection recurrence after liver transplantation. Am J Transpl. 2009;9:1591–601.
61. Kato T, Date T, Miyamoto M, Zhao Z, Mizokami M, Wakita T. Nonhepatic cell lines HeLa and 293 support efficient replication of the hepatitis C virus genotype 2a subgenomic replicon. J Virol. 2005;79:592–6.
62. Fletcher NF, Yang JP, Farquhar MJ, Hu K, Davis C, He Q, et al. Hepatitis C virus infection of neuroepithelioma cell lines. Gastroenterology. 2010;139:1365–74.
63. Fukuhara T, Kambara H, Shiokawa M, Ono C, Katoh H, Morita E, et al. Expression of microRNA miR-122 facilitates an efficient replication in nonhepatic cells upon infection with hepatitis C virus. J Virol. 2012;86:7918–33.

64. Jiang J, Luo G. Apolipoprotein E but not B is required for the formation of infectious hepatitis C virus particles. J Virol. 2009;83:12680–91.
65. Mancone C, Steindler C, Santangelo L, Simonte G, Vlassi C, Longo MA, et al. Hepatitis C virus production requires apolipoprotein A-I and affects its association with nascent low-density lipoproteins. Gut. 2010;60:378–86.
66. Miyanari Y, Atsuzawa K, Usuda N, Watashi K, Hishiki T, Zayas M, et al. The lipid droplet is an important organelle for hepatitis C virus production. Nat Cell Biol. 2007;9:1089–97.
67. Dragic T, Litwin V, Allaway GP, Martin SR, Huang Y, Nagashima KA, et al. HIV-1 entry into CD4+ cells is mediated by the chemokine receptor CC-CKR-5. Nature. 1996;381:667–73.
68. Tatsuo H, Ono N, Tanaka K, Yanagi Y. SLAM (CDw150) is a cellular receptor for measles virus. Nature. 2000;406:893–7.
69. Yanagi Y, Takeda M, Ohno S. Measles virus: cellular receptors, tropism and pathogenesis. J Gen Virol. 2006;87:2767–79.
70. Pileri P, Uematsu Y, Campagnoli S, Galli G, Falugi F, Petracca R, et al. Binding of hepatitis C virus to CD81. Science. 1998;282:938–41.
71. Scarselli E, Ansuini H, Cerino R, Roccasecca RM, Acali S, Filocamo G, et al. The human scavenger receptor class B type I is a novel candidate receptor for the hepatitis C virus. EMBO J. 2002;21:5017–25.
72. Evans MJ, von Hahn T, Tscherne DM, Syder AJ, Panis M, Wolk B, et al. Claudin-1 is a hepatitis C virus co-receptor required for a late step in entry. Nature. 2007;446:801–5.
73. Ploss A, Evans MJ, Gaysinskaya VA, Panis M, You H, de Jong YP, et al. Human occludin is a hepatitis C virus entry factor required for infection of mouse cells. Nature. 2009;457:882–6.
74. Michta ML, Hopcraft SE, Narbus CM, Kratovac Z, Israelow B, Sourisseau M, et al. Species-specific regions of occludin required by hepatitis C virus for cell entry. J Virol. 2010;84:11696–708.
75. Dorner M, Horwitz JA, Robbins JB, Barry WT, Feng Q, Mu K, et al. A genetically humanized mouse model for hepatitis C virus infection. Nature. 2011;474:208–11.
76. Tani H, Komoda Y, Matsuo E, Suzuki K, Hamamoto I, Yamashita T, et al. Replication-competent recombinant vesicular stomatitis virus encoding hepatitis C virus envelope proteins. J Virol. 2007;81:8601–12.
77. Hamamoto I, Nishimura Y, Okamoto T, Aizaki H, Liu M, Mori Y, et al. Human VAP-B is involved in hepatitis C virus replication through interaction with NS5A and NS5B. J Virol. 2005;79:13473–82.
78. Foster TL, Gallay P, Stonehouse NJ, Harris M. Cyclophilin A interacts with domain II of hepatitis C virus NS5A and stimulates RNA binding in an isomerase-dependent manner. J Virol. 2011;85:7460–4.
79. Okamoto T, Nishimura Y, Ichimura T, Suzuki K, Miyamura T, Suzuki T, et al. Hepatitis C virus RNA replication is regulated by FKBP8 and Hsp90. EMBO J. 2006;25:5015–25.
80. Schwartz RE, Trehan K, Andrus L, Sheahan TP, Ploss A, Duncan SA, et al. Modeling hepatitis C virus infection using human induced pluripotent stem cells. Proc Natl Acad Sci USA. 2012;109:2544–8.
81. Wu X, Robotham JM, Lee E, Dalton S, Kneteman NM, Gilbert DM, et al. Productive hepatitis C virus infection of stem cell-derived hepatocytes reveals a critical transition to viral permissiveness during differentiation. PLoS Pathog. 2012;8:e1002617.

Biomaterials 35 (2014) 3416–3426

Contents lists available at ScienceDirect

Biomaterials

journal homepage: www.elsevier.com/locate/biomaterials

Targeted gene delivery by polyplex micelles with crowded PEG palisade and cRGD moiety for systemic treatment of pancreatic tumors

Zhishen Ge [a,g,1], Qixian Chen [a,1], Kensuke Osada [b,f,**], Xueying Liu [c], Theofilus A. Tockary [a], Satoshi Uchida [c], Anjaneyulu Dirisala [b], Takehiko Ishii [b], Takahiro Nomoto [b], Kazuko Toh [c], Yu Matsumoto [c], Makoto Oba [d], Mitsunobu R. Kano [e], Keiji Itaka [c], Kazunori Kataoka [a,b,c,*]

[a] Department of Materials Engineering, Graduate School of Engineering, The University of Tokyo, 7-3-1 Hongo, Bunkyo-ku, Tokyo 113-8656, Japan
[b] Department of Bioengineering, Graduate School of Engineering, The University of Tokyo, 7-3-1 Hongo, Bunkyo-ku, Tokyo 113-8656, Japan
[c] Center for Disease Biology and Integrative Medicine, Graduate School of Medicine, The University of Tokyo, 7-3-1 Hongo, Bunkyo-ku, Tokyo 113-0033, Japan
[d] Department of Molecular Medicinal Sciences, Division of Pharmaceutical Chemistry, School of Pharmaceutical Sciences, Nagasaki University, 1-14 Bunkyo-machi, Nagasaki 852-8521, Japan
[e] Department of Pharmaceutical Biomedicine, Graduate School of Medicine, Dentistry, and Pharmaceutical Sciences, Okayama University, 1-1-1 Tsuhima-Naka, Kita-ku, Okayama 700-8530, Japan
[f] Japan Science and Technology Agency, PRESTO, Japan
[g] CAS Key Laboratory of Soft Matter Chemistry, Department of Polymer Science and Engineering, University of Science and Technology of China, Hefei 230026, China

ARTICLE INFO

Article history:
Received 30 October 2013
Accepted 22 December 2013
Available online 15 January 2014

Keywords:
DNA
Micelle
Nanoparticle
Gene transfer
In vitro test
In vivo test

ABSTRACT

Adequate retention in systemic circulation is the preliminary requirement for systemic gene delivery to afford high bioavailability into the targeted site. Polyplex micelle formulated through self-assembly of oppositely-charged poly(ethylene glycol) (PEG)-polycation block copolymer and plasmid DNA has gained tempting perspective upon its advantageous core–shell architecture, where outer hydrophilic PEG shell offers superior stealth behaviors. Aiming to promote these potential characters toward systemic applications, we strategically introduced hydrophobic cholesteryl moiety at the ω-terminus of block copolymer, anticipating to promote not only the stability of polyplex structure but also the tethered PEG crowdedness. Moreover, M_w of PEG in the PEGylated polyplex micelle was elongated up to 20 kDa for expecting further enhancement in PEG crowdedness. Furthermore, cyclic RGD peptide as ligand molecule to integrin receptors was installed at the distal end of PEG in order for facilitating targeted delivery to the tumor site as well as promoting cellular uptake and intracellular trafficking behaviors. Thus constructed cRGD conjugated polyplex micelle with the elevated PEG shielding was challenged to a modeled intractable pancreatic cancer in mice, achieving potent tumor growth suppression by efficient gene expression of antiangiogenic protein (sFlt-1) at the tumor site.

1. Introduction

Significant advance in nanotechnology-based biomaterials has inspired to develop smart nano-devices to seek the breakthrough of medical care, highlighted as nanomedicine. These medical nano-devices, which are fabricated according to versatile chemistry-based engineering to achieve specific functionalities, have dramatically improved medical diagnosis and treatment [1–4]. One of intriguing example is a gene delivery carrier, which is defined as nanoparticles embedded with genomic materials for targeted delivery to the pathological site and exert functional protein expression with the consequence of restoring normal conditions [5].

* Corresponding author. Department of Materials Engineering, Graduate School of Engineering, The University of Tokyo, 7-3-1 Hongo, Bunkyo-ku, Tokyo 113-8656, Japan. Tel.: +81 3 5841 7138; fax: +81 3 5841 7139.
** Corresponding author. Department of Bioengineering, Graduate School of Engineering, The University of Tokyo, 7-3-1 Hongo, Bunkyo-ku, Tokyo 113-8656, Japan. Tel.: +81 3 5841 1654; fax: +81 3 5841 7139.
E-mail addresses: osada@bmw.t.u-tokyo.ac.jp (K. Osada), kataoka@bmw.t.u-tokyo.ac.jp (K. Kataoka).
[1] These two authors contributed equally to this work.

0142-9612/$ – see front matter © 2013 Elsevier Ltd. All rights reserved.
http://dx.doi.org/10.1016/j.biomaterials.2013.12.086

To realize this concept of gene therapy through systemic administration, the stabilities of gene delivery carriers in blood circulation so as to increase delivery efficiency to the targeted sites are of crucial importance for ultimate therapeutic potency. In order to attain adequate longevity in the harsh biological environment, gene delivery carrier must circumvent an ensemble of predefined biological interferences including enzymatic degradation, protein adsorption and opsonization followed by reticuloendothelial (RES) system capture [6], thereby development of a gene delivery carrier with stealth surface character along with substantial structural stabilities is imperative for systemic use. In view of these requirements, we developed a promising polyplex micelle by self-assemble of block copolymer poly(ethylene glycol) (PEG)-poly{N′-[N-(2-aminoethyl)-2-aminoehtyl]aspartamide} [PAsp(DET)] and plasmid DNA (pDNA) through electrostatic interaction, which has demonstrated considerable therapeutic potential with respect to both safety and efficiency concerns, relying largely on the tempting features of efficient transfection activity and bio-degradable nature from PAsp(DET) [7–10]. The PEG in the block copolymer also plays a crucial role in the polyplex micelle as a protective palisade, which diminishes non-specific interactions with biological components, accounting for stealthiness in the biological condition [6,11–15]. Nevertheless, the systemic use of this system was limited by its insufficient retention in the blood circulation [16], thereby motivating adaptation of this system with strengthened PEG palisade to obtain improved stealthiness for persistence in the bloodstream. Very recently, we established method to quantify PEG crowdedness for polyplex micelles, and recognized importance of increasing crowdedness of PEG palisade in avoiding blood clearance related to RES capture, which is initiated by opsonin adsorption [17]. Prolonged blood retention was observed for polyplex micelle possessing crowded PEG shell characterized as squeezed conformation, whereas those micelles possessing PEG shell characterized by mushroom conformation were cleared from blood compartment at the early stage, validating a worthy strategy of modulation of PEG to high crowdedness for prolonging blood retention. In designing polyplex micelle with elevated PEG crowdedness, energetic description in regulating structure of polyplex micelle should present a rational strategy. To this point, we have clarified DNA condensation is a counterbalance between compaction force from minimization of surface energy by reducing contact area of pDNA/polycation complex and water molecules, and anti-compaction force from PEG steric repulsion, including osmotic pressure from crowded PEG palisade and entropic elasticity derived from restricted conformation and additionally rigidity of folded DNA bundle [17]. Learning from this description, hydrophobic cholesteryl moiety was introduced at the ω-terminus of the block copolymer with the intention of increasing hydrophobicity of complex core. We expected the increased hydrophobicity provides additional compaction force to condense DNA more, which can prevail PEG steric repulsion, eventually promoting PEG for further crowding. Apparently, the increased hydrophobicity of complex is also expected to stabilize the complex structure, so that preventing polyplex micelle from dissociation in the biological condition. Furthermore, in view of a previous finding that the PEG shielding effect was more pronounced with the use of longer PEG (17 kDa rather than 12 kDa), as evidenced by reduced affinity to the cellular membrane [18], 20-kDa PEG was introduced into a PEG-PAsp(DET)-cholesteryl system. To counter the reduced cellular uptake resulting from enhanced PEG shielding by virtue of above-mentioned strategies, we installed a cyclic RGD (Arg-Gly-Asp) peptide (cRGD) at the distal end of PEG. This modification was expected to enhance cellular uptake while prompting the accumulation of polyplex micelle into tumor angiogenic endothelial cells and malignant tumor cells, which feature with the overexpression of $\alpha_v\beta_3$ and $\alpha_v\beta_5$ integrins as cRGD receptors on the cell surface [19–21]. We note that a previous study has indicated that the benefits of ligand conjugation were particularly pronounced for polyplex micelles with high PEG shielding, for which non-specific interaction was minimized so that ligand efficacy elicited and eventually afforded efficient gene expression activity in the transfected cells. In this regard, the polyplex micelle with 20-kDa PEG may hold tempting perspective in fully exploiting benefits of ligand-integrin-mediated affinity to produce high gene expression activity after systemic administration. The current research intends to highlight the impact of PEG elongation upon cholesteryl-stabilized polyplex micelle to pursue prolonged circulation and to emphasize the benefits of strategically utilizing ligand cRGD peptide to promote active tumor targeting abilities. Ultimately, we attempted to test the systemic utility of the proposed system for treatment of modeled pancreatic adenocarcinoma in mice using BxPC3 cells, which is fibrotic and also hard to be treated with conventional chemotherapy [22].

2. Materials and methods

2.1. Materials

α-Methoxy-ω-amino-PEG (M_w 12,000 and 20,000) and α-acetal-ω-amino-PEG (M_w 20,000) were obtained from NOF Co., Ltd. (Tokyo, Japan). β-Benzyl-L-aspartate N-carboxyanhydride (BLA-NCA) was obtained from Chuo Kaseihin Co., Inc. (Tokyo, Japan). Diethylenetriamine (DET), cholesterol, n-butylamine, and trifluoroacetic acid were purchased from Wako Pure Chemical Industries, Ltd. 4-Dimethylaminopyridine (DMAP) and dicyclohexylcarbodiimide (DCC) were purchased from Aldrich Chemical Co. Ltd. (Milwaukee, WI). Other chemicals were used as received. The cRGDfK-ε-caproic acid-cysteine (cRGD peptide) was purchased from Peptide Institute Inc. (Osaka, Japan). Alexa680 succinimidyl ester was a product of Invitrogen (Carlsbad, CA). Fetal bovine serum (FBS) was purchased from Dainippon Sumitomo Parma Co., Ltd. (Osaka, Japan). pDNAs, pBR322 (4361 bp) and pGL3 control vector (5256 bp) were purchased from Takara Bio Inc. (Otsu, Japan). The pDNA encoding luciferase with a CAG promoter provided by RIKEN Gene Bank (Tsukuba, Japan) was amplified in competent DH5α *Escherichia coli* and purified with a QIAGEN HiSpeed Plasmid MaxiKit (Germantown, MD). Cell culture lysis buffer and luciferase Assay System Kit was purchased from Promega Co. (Madison, WI). The Micro BCA™ Protein Assay Reagent Kit was purchased from Pierce Co., Inc. (Rockford, IL). The pDNA encoding a soluble form of vascular endothelial growth factor (VEGF) receptor-1 (sFlt-1) was provided by Prof. Masabumi Shibuya at Jobu University, and was prepared as previously reported [16]. Dulbecco's modified Eagle's medium (DMEM) was purchased from Sigma–Aldrich (St. Louis, MO). For cellular uptake and intracellular distribution assay, pDNA was labeled with Cy5 using a Label IT Nucleic Acid Labeling Kit from Mirus Bio Corporation (Madison, WI) according to the manufacturer's protocol. Human pancreatic cancer BxPC3 cells were obtained from the American Type Culture Collection (Manassas, VA). BALB/c nude mice (female, 5 weeks old) were purchased from Charles River Laboratories (Tokyo, Japan). All animal experimental protocols followed the guidelines of the Animal Committee of the University of Tokyo.

2.2. Polymer synthesis

The procedures for synthesis of block copolymers, PEG-PAsp(DET)-cholesteryl and cRGD-PEG-PAsp(DET)-cholesteryl are presented in Scheme S1 of Supporting Information. Cholesteryl bearing a reactive carboxyl group was prepared from substitution of 3-hydroxyl group in cholesterol to a primary amine, followed by reaction with succinic anhydride (Detailed procedure is described in Supporting Information). The precursor block copolymer PEG-poly(β-benzyl-L-aspartate) (PEG-PBLA) was prepared according to a ring-opening polymerization scheme as previously reported [7]. The polymerization of monomer BLA-NCA was initiated from the ω-NH_2 terminal group of α-methoxy-ω-amino-PEG to obtain PEG-PBLA. The terminal amino group of PBLA segment was then coupled with the carboxyl group of cholesteryl in the presence of DCC (10 eq) and DMAP (2 eq) in DMF for an overnight reaction. The resulting polymer was purified by precipitation into mixture of chilled diethyl ether and isopropanol (*v*:*v* = 2:1) thrice and lyophilized from benzene to obtain PEG-PBLA-cholesteryl. Then, an aminolysis reaction was performed to introduce diaminoethane moiety into the side chain of PBLA for PEG-PAsp(DET)-cholesteryl. For synthesis of cRGD-PEG-PAsp(DET)-cholesteryl, acetal-PEG-NH_2 was used as a starting material for polymerization, followed by a similar synthetic procedure to prepare acetal-PEG-PAsp(DET)-cholesteryl with only minor modifications in the purification process after aminolysis. The reaction mixture was added dropwise to a chilled mixture of diethyl ether and ethanol (*v*:*v* = 7:3, also containing acetic acid to neutralize DET) for precipitation to obtain the crude product of acetal-PEG-PAsp(DET)-cholesteryl. The precipitated product was further

purified by sequential vacuum drying and dialysis against acetate buffer for thrice and deionized water for thrice at 4 °C. The proposed purification procedures were applied to prevent the conversion of the acetal to be reactive. The acetal-PEG-PAsp(DET)-cholesteryl product was dissolved in water and the solution was adjusted to pH 2 using HCl for conversion of acetal group to be reactive with cRGD peptide (10 eq to the block copolymer). Note that cRGD peptide was prior dissolved in $NaHCO_3$ buffer (0.1 M, pH 7.4) containing dithiothreitol (10 eq to peptide) to cleave the potential disulfide bond between the cysteine termini. After 1 h of incubation, cRGD peptide solution was added into the acetal-PEG-PAsp(DET)-cholesteryl block copolymer solution, followed by adjusting pH to 5 for overnight reaction at 4 °C. The final product cRGD-PEG-PAsp(DET)-cholesteryl was obtained after dialysis against 1 M NaCl solution (thrice) and dialysis against deionized water (thrice) at 4 °C. The dialyzed product solution was lyophilized to yield the final product as a chloride salt form. The prepared polymers were determined to have a narrow unimodal molecular weight distribution by gel permeation chromatography (Supporting Information Fig. S3). The polymerization degree of the PAsp(DET) segment, efficiencies of cholesteryl and cRGD conjugation was determined from the ^1H NMR spectra in D_2O at 25 °C (Table 1).

2.3. Preparation of polyplex micelles

Synthesized block copolymers were dissolved in 10 mM HEPES buffer (pH 7.4) as stock solutions. Aliquot of polymer solution was added to pDNA solution for complexation at varying N/P ratios (molar ratio of amino groups in polymer to phosphate groups in pDNA), followed by overnight incubation at 4 °C. The final concentration of pDNA in all the samples was adjusted to 33.3 μg/mL for *in vitro* experiments and 100 μg/mL for *in vivo* experiments. Note that all the pre-experimental procedures involving with polymer solution or complex solution were strictly carried out at low temperature, under 4 °C refrigeration or in an ice bath to avoid polymer fragmentation [9].

2.4. Cellular uptake

Cellular uptake efficiency was evaluated by flow cytometry (BD LSR II, BD, Franklin Lakes, NJ). Cy5-labeled pDNA was used to prepare a group of polyplex micelles. HeLa cells were seeded on a 6-well culture plate (100,000 cells/well) and incubated for 24 h in 2 mL of DMEM containing 10% FBS in a humidified atmosphere with 5% CO_2 at 37 °C. The medium was replaced with fresh medium, followed by addition of 150 μL polyplex micelle solution (33.3 μg pDNA/mL) into each well. After 24 h incubation, the cells were washed thrice with PBS to remove extracellular Cy5 fluorescence. After detachment of cells from the culture plate with trypsin, the cells were harvested and re-suspended in PBS for flow cytometry measurement.

2.5. In vitro gene expression

HeLa cells were seeded on 24-well culture plates (20,000 cells/well) and incubated for 24 h in 400 μL of DMEM containing 10% FBS in a humidified atmosphere with 5% CO_2 at 37 °C. The medium was replaced with 400 μL of fresh medium, followed by addition of 30 μL each polyplex micelle solution (1 μg pDNA/well). After 24 h of incubation, the medium was replaced with 400 μL fresh DMEM, followed by another 24 h of incubation. The cells were washed with 400 μL of PBS, and lysed in 150 μL of the cell culture lysis buffer. The luciferase activity of the lysates was evaluated from the photoluminescence intensity using Mithras LB 940 (Berthold Technologies, Bad Wildbad, Germany). The measured luciferase activity was normalized according to corresponding amount of proteins in the lysates determined by the Micro BCA™ Protein Assay Reagent Kit.

2.6. Intracellular distribution

The endosome entrapment ratio was determined by evaluating colocalization degree of pDNA and endosomes by confocal laser scanning microscopy (CLSM). In brief, Cy5-labeled pDNA was used to prepare a class of polyplex micelles at N/P 8. HeLa cells (50,000 cells) were seeded on 35-mm cell culture dishes and incubated for 24 h in 1 mL of DMEM containing 10% FBS. The medium was replaced with fresh medium, followed by the addition of 75 μL of polyplex micelle solution (33.3 μg pDNA/mL) into each cell culture dishes. After 24 h of incubation, the medium was removed and the cells were rinsed thrice with PBS prior to the imaging. The intracellular distribution of each polyplex micelle was observed by CLSM after staining acidic late endosomes and lysosomes with LysoTracker Green (Molecular Probes, Eugene, OR) and nuclei with Hoechst 33342 (Dojindo Laboratories, Kumamoto, Japan). The CLSM observation was performed using LSM 510 (Carl Zeiss, Germany) with a 63× objective (C-Apochromat, Carl Zeiss, Germany) at excitation wavelengths of 488 nm (Ar laser), 633 nm (He–Ne laser), and 710 nm (MaiTai laser for 2-photon imaging) for LysoTracker Green (green), Cy5 (red), and Hoechst 33342 (blue), respectively. The colocalization ratio was calculated as previously described [10] according to the formula:

$$\text{Colocalization ratio} = \text{number of yellow pixels/number of yellow and red pixels,}$$

where yellow corresponds to the pDNA that is trapped in late endosome/lysosomes, and red corresponds to pDNA in the cytosol.

2.7. Morphology observation

Morphology observation was performed with transmission electron microscopy (TEM) measurement by an H-7000 electron microscope (Hitachi, Tokyo, Japan) operated at 75 kV acceleration voltages for insight on the morphology of polyplex micelles containing pBR322 pDNA at N/P 8. Copper TEM grids with carbon-coated collodion film were glow-discharged for 10 s using an Eiko IB-3 ion coater (Eiko Engineering Co. Ltd., Japan). The grids were dipped into the desired polyplex micelle solution, which was premixed with uranyl acetate (UA) solution (2% (w/v)) for 30 s to stain the DNA. The sample grids were blotted by filter paper to remove excess complex solution, followed by air-drying for 30 min. Note that the PEG shell is invisible under TEM owing to its low affinity with UA. Thus, the DNA in the complex was selectively visualized without interference from PEG moieties surrounding pDNA strands. The obtained TEM image was further analyzed with ImageJ 1.44 (National Institutes of Health) to quantify the length of the major axis in each sample, and more than 100 individual polyplex micelles were measured to obtain rod length distribution.

2.8. Binding numbers of block copolymers to pDNA in polyplex micelles

The binding behaviors of block copolymers to pDNA in each polyplex micelle were investigated according to an ultracentrifuge method [23]. As reported previously, ultracentrifugation of polyplex micelle solution allows selective sedimentation of polyplex micelles, while unbound free polymers remain in the supernatant. In consequence, the binding fraction of polymer can be determined by subtracting free polymer (remaining in the supernatant after sedimentation) from the total fed polymer. To quantify the associating number of block copolymers in the polyplex micelle, Alexa-680 labeled block copolymer (labeling procedures according to protocol provided by the manufacturer, conjugation efficiency 0.5 Alexa-680 molecules per block copolymer) was used to prepare a class of polyplex micelle at N/P 8. After overnight incubation at 4 °C, 500 μL of each polyplex micelle solution was placed into thickwall polycarbonate tube, 343776 (Beckman Coulter, Inc., Fullerton, CA) and subjected to ultracentrifugation (Optima TLX, Beckman Coulter, Inc., Fullerton, CA) equipped with TLA-120.1 rotor for 3 h under 50,000 × *g* for complete sedimentation of polyplex micelles, while the unbound free polymer remained in the upper supernatant. The supernatant containing free block copolymer was collected for absorbance measurement by a UV-Vis spectrometry (ND-3300, NanoDrop, Wilmington, NC) at a wavelength of 680 nm. The concentration of free block copolymer in the supernatant was determined from the obtained absorbance according to a calibration curve from Alexa680-labeled block copolymer solutions.

2.9. Stability in blood circulation

Polyplex micelles prepared from CAG-Luc2 were intravenously administered into blood stream. After an appropriate time (5 min, 10 min, 15 min and 30 min), the blood samples were collected and the remaining pDNA in the blood was purified and extracted with a DNeasy blood and tissue kit (QIAGEN, Germantown, MD) according to the protocol provided by the manufacture. Quantification of pDNA was obtained by real time polymerase chain reaction (RT-PCR) measurement by using the ABI 7500 Fast Real-time RT-PCR System (Applied Biosystems, Foster City, CA) with forward primer TGCAAAAGATCCTCAACGTG and reverse primer AATGGGAAGTCACGAAGGTG. The remaining pDNA in the blood stream was expressed as the percentage of pDNA dosage.

Table 1
A series of synthesized block copolymers.

Polymers	PEG M_w	PAsp (DET) DP[a]	Abbreviation	Cholesteryl group [%]	cRGD [%]	M_w/M_n[b]
PEG_{272}-$PAsp(DET)_{53}$	12,000	53	PEG12	0	0	1.05
PEG_{272}-$PAsp(DET)_{61}$-cholesteryl	12,000	61	PEG12C	87	0	1.04
PEG_{454}-$PAsp(DET)_{60}$-cholesteryl	20,000	60	PEG20C	89	0	1.07
cRGD-PEG_{454}-$PAsp(DET)_{57}$-cholesteryl	20,000	57	R-PEG20C	86	39	1.06

[a] DP: polymerization degree of PAsp(DET) segment.
[b] M_w/M_n was determined from the precursor of each block copolymer before aminolysis according to calibration with differing M_w of PEG as standards.